POINT-SCATTERER FORMULATION OF TERRAIN CLUTTER STATISTICS

G. R. Valenzuela, et al

Naval Research Laboratory
Washington, D. C.

27 September 1972

AD 750668

Security Classification

DOCUMENT CONTROL DATA - R & D

Security classification of title, body of abstract and indexing annotation must be entered when the overall report is classified)

1. ORIGINATING ACTIVITY (Corporate author) Naval Research Laboratory Washington, D.C. 20390	2a. REPORT SECURITY CLASSIFICATION Unclassified 2b. GROUP

3. REPORT TITLE

POINT-SCATTERER FORMULATION OF TERRAIN CLUTTER STATISTICS

4. DESCRIPTIVE NOTES (Type of report and inclusive dates)
This is a final report on one phase of the problem; work on other phases is continuing

5. AUTHOR(S) (First name, middle initial, last name)

G. R. Valenzuela and M. B. Laing

6. REPORT DATE	7a. TOTAL NO. OF PAGES	7b. NO. OF REFS
September 27, 1972	48	17

8a. CONTRACT OR GRANT NO. NRL Problem R02-37 b. PROJECT NO. A310310B/652A/2 R02101-002 c. d.	9a. ORIGINATOR'S REPORT NUMBER(S) NRL Report 7459 9b. OTHER REPORT NO(S) (Any other numbers that may be assigned this report)

10. DISTRIBUTION STATEMENT

Approved for public release; distribution unlimited.

11. SUPPLEMENTARY NOTES	12. SPONSORING MILITARY ACTIVITY
	Department of the Navy (Naval Air Systems Command) Washington, D.C. 20360

13. ABSTRACT

The first-order statistics of terrain clutter are investigated theoretically and experimentally. The return from a point-scatterer (a scintillating signal) is used as a basis for generating the statistical properties of terrain clutter as observed by side-looking airborne radars. According to the model the limiting distributions of terrain clutter are the Gaussian distribution and the distribution for a scintillating signal (specular clutter). An array of point-scatterers within the radar beam produces clutter which has long tails similar to those of a lognormal distribution.

The convergence of the first-order statistics of a scintillating signal to the statistics of a sinusoidal signal is demonstrated. This property allows the use of many statistical results available in statistical communication for sine waves in Gaussian noise to interpret and predict in many cases the statistical properties of terrain clutter.

Also, the statistics of terrain clutter are inferred from data taken with the Naval Research Laboratory's Four Frequency Radar System by the Kolmogorov—Smirnov test of the cumulative distribution and by the computation of the first five central moments of the normalized radar cross section of terrain (in decibels). It is found that in general, terrain clutter statistics is not exponential (with Rayleigh envelope) nor lognormal distributed, which supports some of the predictions of the analytical results.

DD FORM 1 NOV 68 1473 (PAGE 1)

S/N 0101-807-6801

Security Classification

Security Classification

14 KEY WORDS	LINK A		LINK B		LINK C	
	ROLE	WT	ROLE	WT	ROLE	WT
Terrain clutter						
Statistical model						
Point scatterers						
Gaussian clutter						
Lognormal clutter						
Distribution function						
Density function						
Kolmogorov-Smirnov test						
Independent samples						
Central moments						
Side-looking radar						

CONTENTS

Abstract ii
Problem Status ii
Authorization ii

INTRODUCTION 1

STATISTICAL PROPERTIES OF SCINTILLATING SIGNALS .. 2

Scattering Considerations 2
One Scintillating Signal 4
Central Limit Theorem 7
Many Scintillating Signals 10

STATISTICS OF THE ENVELOPE 13

INFERENCE OF THE STATISTICS OF TERRAIN CLUTTER .. 16

The Distribution Function 17
The Central Moments 17

RESULTS AND CONCLUSIONS 22

ACKNOWLEDGMENTS 43

REFERENCES 43

POINT-SCATTERER FORMULATION OF TERRAIN CLUTTER STATISTICS

INTRODUCTION

Through the years terrain clutter has remained as the main limitation of airborne radars in the detection of targets when operating over land. To describe terrain clutter in a more realistic manner and help radar designers and analysts to make provisions for the large probability of false alarms obtained in this environment, many attempts have been made to understand the basic phenomena responsible for this clutter and then be in a position to predict the effects of terrain clutter on the radar systems.

Presently, it is pretty well accepted that terrain clutter is the result of two basic mechanisms (1,2): strong point-scatterers (or speculars) and a Gaussian-distributed clutter of Rayleigh-distributed envelope, which is produced by many equal-amplitude scatterers.

In previous statistical investigations, a priori statistics (e.g., lognormal, Rayleigh, Chi-Square and Rician) known to occur in terrain clutter have been used from the outset to describe the process. Here, a much more fundamental point of view has been taken. The complete process is developed in terms of the statistical properties of the scintillating return from the elementary point-scatterer, and the more complicated distributions can be obtained by a superposition of many point-scatterers within the radar beam. Although the basic idea is quite general, in this investigation it will be applied for the particular case of a side-looking radar.

With the point-scatterer as the building block of the clutter process, a great deal of physical insight can be obtained and terrain clutter data may be interpreted from a more fundamental point of view. For example, point-scatterers in many instances can be identified in a topographic map or in a more precise manner by means of synthetic aperture maps obtained at the same radar frequency. That is, they are in most cases physical entities which appear in the form of various natural terrain features or man-made objects. In the analytical investigation it is proved that the first-order statistics of a scintillating signal (i.e., a linear frequency-modulated signal produced by a point-scatterer as the airborne radar flies by) converge asymptotically to the first-order statistics of a sinusoidal signal, or more precisely they converge in density and distribution to the statistics of a sinusoid for large frequency modulation rates and large observation times.

Analytical expressions are derived for the first-order statistics of a scintillating signal using the assumption that its frequency spectrum is constant within the time of the frequency sweep. In the more realistic case in which several point-scatterers appear within the resolution cell, it is not possible to obtain explicit analytical expressions for the first-order statistics of the return. In those cases, the statistics may be obtained by convenient computer simulation or by invoking the asymptotic property of the statistics of a scintillating signal. In many cases it is possible to obtain a good deal of insight by proper interpretation of available statistical results for sine waves and Gaussian noise. Many of the

statistical properties for the envelope of terrain clutter may be obtained in a similar manner.

The convergence of the statistics of the sum of n sine waves, of irrational periods of the same amplitude, to the Gaussian distribution is of order $1/n$ as $n \to \infty$. However, the convergence of the statistics of n scintillating signals of equal amplitude should be of order $1/\sqrt{n}$ or slower, since the mean value of scintillating signals is nonzero and the component signals are not independent. The slower convergence of the statistics of the sum of n scintillating signals may be directly responsible for the lognormal statistical properties of clutter which sometimes are observed in terrain clutter.

Finally, the statistics of terrain clutter obtained with the Four Frequency Radar (4 FR) system are obtained. The empirical investigation shows that in general terrain clutter is neither Gaussian (with an exponentially distributed radar cross section) nor lognormal. These conclusions have been arrived at by means of a Kolmogorov-Smirnov test of the cumulative distribution of the normalized radar cross section (NRC) of terrain and by an investigation of the first five central moments of the NRC. As a general rule the type of terrain is reflected most markedly in the mean value of the NRC.

STATISTICAL PROPERTIES OF SCINTILLATING SIGNALS

Scattering Considerations

Consider an airborne, side-looking, coherent pulsed radar system illuminating the terrain at small depression angles; see Fig. 1. In such a scattering configuration, the range resolution is determined by the radar pulse width and the azimuthal resolution is a function of the horizontal dimensions of the antenna (3).

The radar transmits a characteristics spectrum of electromagnetic plane waves which are scattered by the terrain in all directions. The backscattered waves are collected by the radar receiver and they constitute the terrain clutter, whose statistical properties we are interested in determining.

We will be dealing with the simplest form as possible of the backscattered signal in order to include only the necessary features of the return containing information on the physical process responsible for terrain clutter. For our purpose, the return from a point-scatterer within the resolution cell will be of the complex form

$$Y(t) = \frac{A(t)}{R(t)} e^{i\phi(t)} e^{-i\omega_0 t} \qquad \text{for } 0 \leq t \leq T, \tag{1}$$

keeping in mind that we are interested in the real part of $Y(t)$. The continuous wave (CW) version of the backscattered signal about the angular frequency ω_0 will be used for simplicity. $A(t)$ contains both the amplitude weight of the two-way antenna radiation pattern and the intrinsic amplitude of the scatterer, $R(t) = \sqrt{(R_0^2 + v^2t^2)}$ is the slant range to the scatterer, $\phi(t) = 2\beta R(t)$ is the phase, v is the speed of the aircraft, $\beta = 2\pi/\lambda$ is the propagation constant of a plane wave transmitted by the radar, and T is the observation time dependent on the antenna beamwidth. In many practical cases $vt << R_0$, R_0 being the slant range from the radar to the point-scatterer at broadside. The return signal for these cases can be approximated by

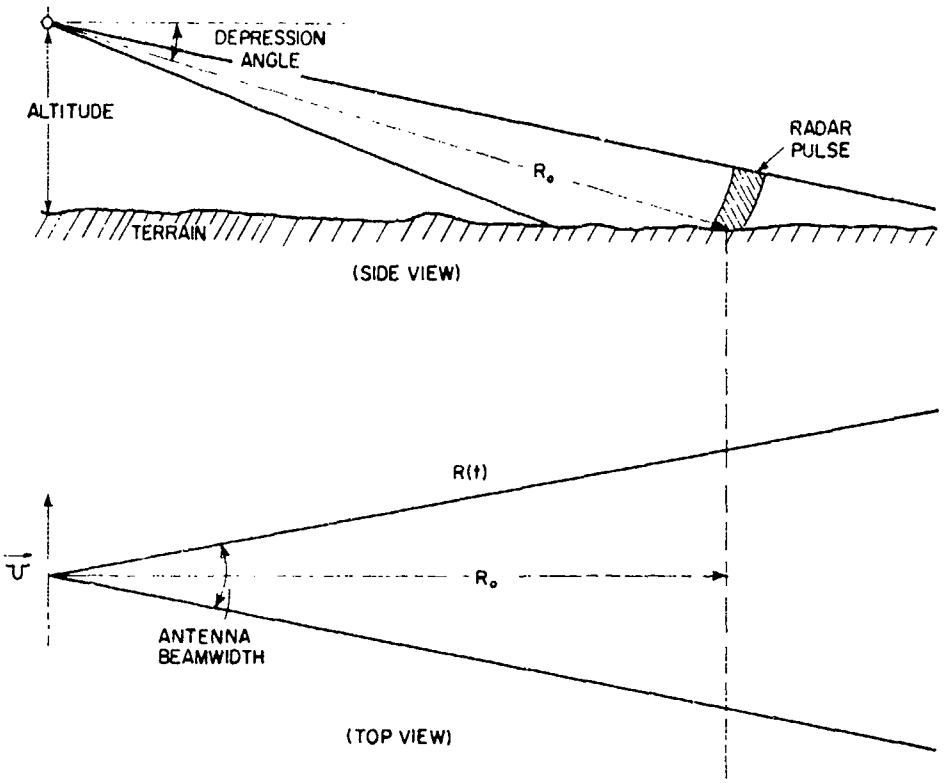

Fig. 1—Scattering geometry for a side-looking radar

$$Y(t) = \frac{A(t)}{R_0} e^{i(\phi_0 + Kt^2)} e^{-i\omega_0 t}, \tag{2}$$

where $\phi_0 = 2\beta R_0$ and $K = \beta v^2/R_0$, which is the scintillating rate. For $t < 0$, Eqs. (1) and (2) will apply if we let $\phi(t) = -\phi(-t)$, since the rate of change of slant range in this case is negative. For our purpose we will deal with the return for $t > 0$ only, since by itself it contains all the intrinsic properties of the return.

Thus, terrain clutter may be represented as the superposition of a great number of scintillating signals at any given time

$$Y(t) = e^{-i\omega_0 t} \sum_{k=1}^{n} a_k e^{i\phi_k + iK(t-t_k)^2} \qquad \text{for } 0 \leq t \leq T, \tag{3}$$

and for simplicity all amplitude effects have been lumped into the a_k coefficients which are taken to be constants.

Thus, in fact, tacitly we are assuming that the illumination pattern of the radar antenna is independent of angle of uniform weight. The scintillating rate K and the phases ϕ_k are also assumed to be constant. This is really a simplification because in practice the amplitude, the phases, and even the number of scatterers producing the return may change within the observation time T.

One Scintillating Signal

In what follows we will deal with a coherently detected version of the scintillating signal of Eq. (1). The fluctuations in this case appear about zero frequency.

$$Y(t) = A \cos (Kt^2 + \phi) \qquad \text{for} \quad 0 \leqslant t \leqslant T, \tag{4}$$

which is a linear frequency modulated signal. The frequency spectrum of Eq. (4) is a complicated expression involving Fresnel integrals (4).

In Fig. 2 the frequency spectrum of a scintillating signal, as obtained by Klauder and others, is shown as a function of the parameter KT^2. As $KT^2 \to \infty$, the spectrum of a scintillating signal tends to a constant. In practice the side-looking radars operating at small depression angles KT^2 is large. In this analysis we will asusme that the frequency spectrum of the scintillating signal from a point-scatterer is constant during the observation time. Thus, from elementary probability theory the characteristic function of Eq. (4) can be obtained from

$$F(\xi) = \int_0^{2X_0} e^{i\xi A \cos [(X^2/K)+\phi]} p(X) dX, \tag{5}$$

where

$$X = Kt$$

$$p(X) = \frac{1}{2X_0} = \frac{1}{2KT}.$$

Using the identity

$$e^{iZ\cos\theta} = \sum_{m=0}^{\infty} i^m \epsilon_m J_m(Z) \cos m\theta \tag{6}$$

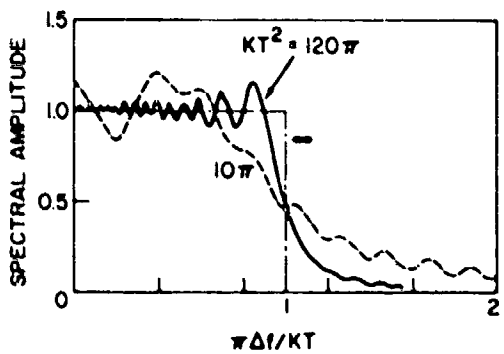

Fig. 2—Frequency spectrum of a linear frequency modulated signal

where $\epsilon_0 = 1$ and $\epsilon_m = 2$ for $m \geqslant 1$, in Eq. (5). By reversing the order of integration and summation, the following expression can be obtained for the characteristic function:

$$F(\xi) = \sum_{m=0}^{\infty} i^m b_m J_m(\xi A), \tag{7}$$

with

$$b_m = \frac{\epsilon_m}{2X_0} \int_0^{2X_0} \cos m\left(\frac{X^2}{K} + \phi\right) dX.$$

By making a change in variables it is simple to show that

$$b_m = \left(\frac{\pi}{2mK}\right)^{1/2} \frac{1}{T} \left\{\cos m\phi\, C(\tau_m) - \sin m\phi\, S(\tau_m)\right\} \qquad \text{for} \quad m \geqslant 1$$

and

$$b_0 = 1,$$

where

$$\tau_m = 2T\left(\frac{2mK}{\pi}\right)^{1/2}$$

with $C(\tau_m)$ and $S(\tau_m)$ being the Fresnel integrals defined by

$$C(\tau_m) = \int_0^{\tau_m} \cos\left(\frac{\pi}{2}\tau^2\right) d\tau$$

and

$$S(\tau_m) = \int_0^{\tau_m} \sin\left(\frac{\pi}{2}\tau^2\right) d\tau.$$

The probability density function (pdf) is by definition the Fourier transform of the characteristic function. After the manipulations we find that

$$p(Y) = \begin{cases} \pi^{-1}(A^2 - Y^2)^{-1/2} \displaystyle\sum_{m=0}^{\infty} (-)^m b_m \cos\left(m \sin^{-1} \frac{Y}{A} + \frac{m\pi}{2}\right), & |Y| \leqslant A \\ 0, & |Y| > A \end{cases} \tag{8}$$

As usual from the pdf, the distribution function can be obtained with no difficulty. It can be shown to be

$$P\{Y > Y\} = \left(\frac{1}{2} - \frac{1}{\pi}\sin\frac{Y}{A}\right) + \frac{1}{\pi}\sum_{m=1}^{\infty}\frac{(-)^{m+1}b_m}{m}\sin\left(m\sin^{-1}\frac{Y}{A} + \frac{m\pi}{2}\right). \quad (9)$$

The mean value of the scintillating signal can be shown to be

$$\text{Mean}\{Y\} = \frac{A}{2T}\left(\frac{\pi}{2K}\right)^{1/2}[\cos\phi\, C(\tau_1) - \sin\phi\, S(\tau_1)]\,. \quad (10)$$

The term in parentheses outside the infinite sum in Eq. (9) is the expression for a sinusoidal signal of amplitude A. Since, in deriving Eqs. (7) through (10) we have assumed that KT^2 is sufficiently large so that the spectrum of the scintillating signal is constant in the interval $(0, 2KT)$, we may replace the Fresnel integrals by their asymptotic value 0.5. Thus, the asymptotic form of Eqs. (8) through (10) are respectively,

$$p(Y) \sim \frac{1}{\pi}(A^2 - Y^2)^{-1/2} + \frac{(A^2 - Y^2)^{-1/2}}{2T\sqrt{\pi K}}\sum_{m=1}^{\infty}\frac{(-)^m}{m^{1/2}}\cos\left(\frac{\pi}{4} + m\phi\right) \quad (11)$$

$$\times \cos\left(m\sin^{-1}\frac{Y}{A} + \frac{m\pi}{2}\right)$$

$$P\{Y > Y\} \sim \left(\frac{1}{2} - \frac{1}{\pi}\sin^{-1}\frac{Y}{A}\right) + \frac{1}{2T\sqrt{\pi K}}\sum_{m=1}^{\infty}\frac{(-)^{m+1}}{m^{3/2}}\cos\left(\frac{\pi}{4} + m\phi\right) \quad (12)$$

$$\times \sin\left(m\sin^{-1}\frac{Y}{A} + \frac{m\pi}{2}\right)$$

and

$$\text{Mean}\{Y\} \sim \frac{A}{4T}\left(\frac{\pi}{K}\right)^{1/2}\cos\left(\frac{\pi}{4} + \phi\right). \quad (13)$$

In Fig. 3, the convergence of the distribution function of a scintillating signal toward the distribution of a sinusoidal signal for increasing values of T is demonstrated. The cumulative distribution for the scintillating signals in the figure were obtained by computer simulation by sampling Eq. (4). The result is in agreement with the prediction of Eq. (12). For example, for $Y = 0$ and $\phi = 0$, Eq. (12) assumes the form

$$P\{Y > 0\} \sim \frac{1}{2} + \frac{1}{2T\sqrt{2\pi K}}\sum_{m=1}^{\infty}\frac{(-)^{m+1}}{(2m-1)^{3/2}}\,. \quad (14)$$

and the numerical value of the infinite sum is 0.865 to three decimals.

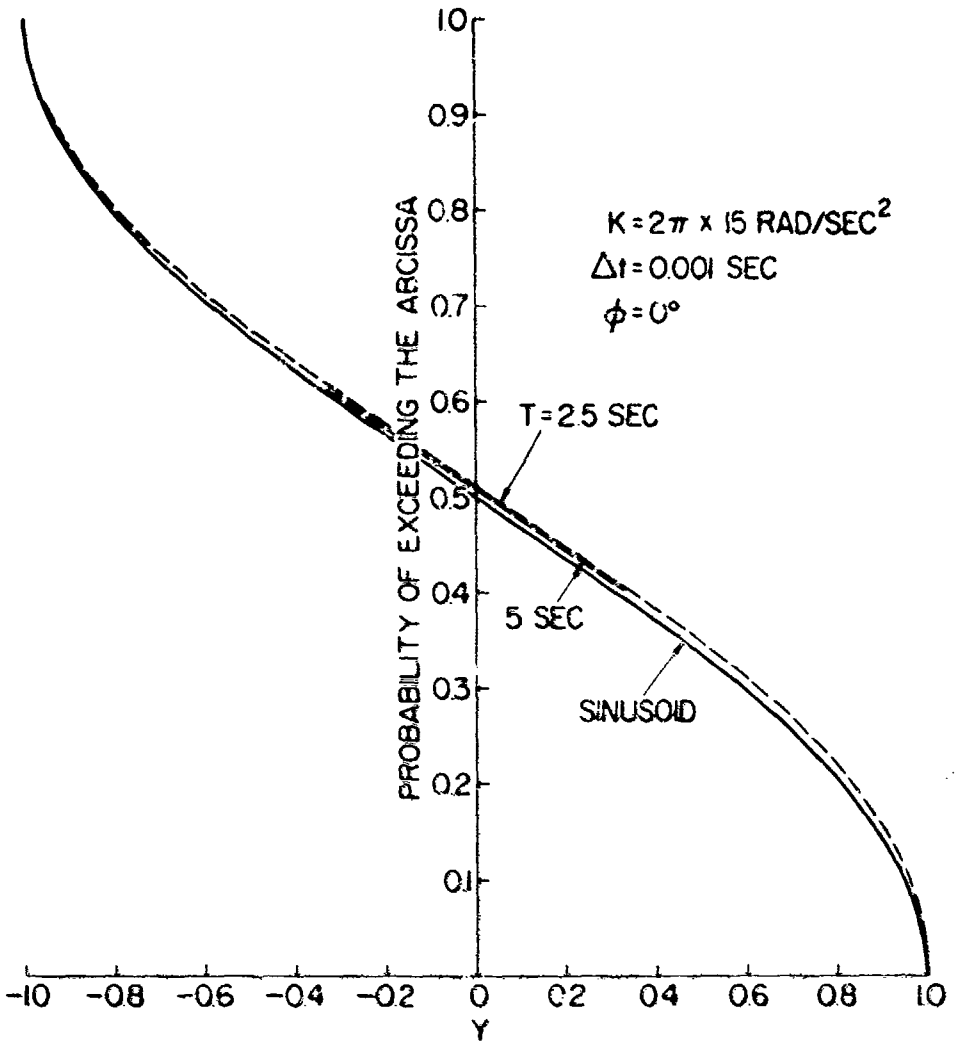

Fig. 3—The distribution of one scintillating signal

Thus, for large $T\sqrt{K}$ factors, the first-order statistics of a scintillating signal are very similar to those for a sine wave and as $T\sqrt{K} \to \infty$ they become the same. However, some important differences exist, for example while the mean value for a sine wave is zero, the mean value for a scintillating signal is nonzero, given by Eq. (13). This difference in the first-order statistics of these two signals yields a different rate of convergence of the first-order statistics for the sum of scintillating signals as compared to that for sine waves (as the number of the components increases), toward the Gaussian distribution. This point is investigated later on.

Central Limit Theorem

As an illustrative example consider the convergence of the distribution of the sum of n sine waves with irrational periods (irrational periods are required so that the sine waves are mutually independent) and amplitudes a_k to the Gaussian distribution. Via the characteristic function it is quite easy to derive the pdf which is of the form (5)

$$p(Y) \sim \frac{1}{\sqrt{2\pi\sigma^2}} e^{-Y^2/2\sigma^2}\left\{1 - \frac{\sum_{k=1}^{n} a_k^4}{64\sigma^4}(t^4 - 6t^2 + 3) + \ldots\right\}, \tag{15}$$

and the distribution function which is given by

$$P\{\mathbf{t} > t\} \sim \frac{1}{2}[1 - \Phi(t)] + \frac{1}{\sqrt{2\pi}} e^{-t^2/2} \frac{\sum_{k=1}^{n} a_k^4}{64\sigma^4}(3t - t^3) + \ldots, \tag{16}$$

where

$$2\sigma^2 = \sum_{k=1}^{n} a_k^2, \quad t = \frac{Y}{\sigma}$$

and

$$\Phi(t) = \sqrt{\frac{2}{\pi}} \int_0^t e^{-X^2/2} dX.$$

The convergence of the density function for the sum of sine waves of the same amplitude toward the Gaussian distribution is illustrated in Fig. 4.

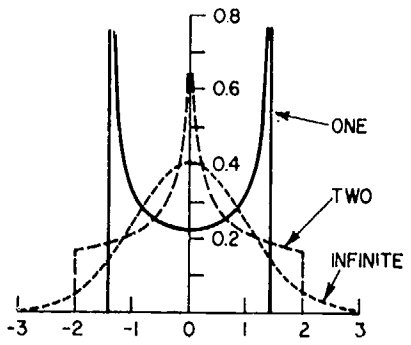

Fig. 4—The density function of the sum of sine waves of equal amplitude and irrational periods

The general convergence problem of the distribution of the sum of n independent random variables to the Gaussian distribution was investigated by Gnedenko and Kolmogorov (6). For the more general case, in which each of the components is distributed according to a different density function, the convergence of the probability density function of the sum to the Gaussian distribution is in the following manner:

$$p(Y) \sim \frac{e^{-Y^2/2M_2}}{\sqrt{2\pi M_2}}\left\{1 + \frac{M_1}{M_2^{1/2}}t - \frac{1}{6}\frac{M_3}{M_2^{3/2}}(3t - t^3)\right. \tag{17}$$

$$\left. + \frac{1}{24}\frac{(M_4 - 3M_2')}{M_2^2}(t4 - 6t^2 + 3) + \ldots\right\}$$

where

$$t = \frac{Y}{\sqrt{M_2}},$$

and

$$P\{\mathbf{t} > t\} \sim \frac{1}{2}[1 - \Phi(t)] + \frac{e^{-t^2/2}}{\sqrt{2\pi}}\left\{\frac{M_1}{M_2^{1/2}} - \frac{1}{6}\frac{M_3}{M_2^{3/2}}(1 - t^2)\right. \tag{18}$$

$$\left. + \frac{1}{24}\frac{(M_4 - 3M_2')}{M_2^2}(t^3 - 3t) + \ldots\right\}$$

for the distribution function, where

$$M_1 = \sum_{k=1}^{n} m_{1k},$$

$$M_2 = \sum_{k=1}^{n} m_{2k},$$

$$M_2' = \sum_{k=1}^{n} m_{2k}^2,$$

$$M_3 = \sum_{k=1}^{n} m_{3k},$$

$$M_4 = \sum_{k=1}^{n} m_{4k},$$

and

$$m_{1k}, m_{2k}, \ldots$$

are the first-order moments of the component random variables.

The net conclusion obtained from examining Eqs. (15) through (18) is that the distribution of the sum of independent random variables with zero mean converges to the Gaussian distribution as $1/n$ with the number of components and when the mean value of the component random variables is nonzero the convergence of the distribution of the sum to the Gaussian distribution is slower, of order $1/\sqrt{n}$.

Bernstein (7) investigated the convergence of the distribution of the sum of dependent random variables. In this case the Central Limit Theorem arguments apply to the number of independent subsets contributing to the sum, which obviously is smaller than the total number of the component random variables.

Many Scintillating Signals

In general, terrain clutter is the result of many point-scatterers within the antenna beam. Analytical expressions for the first-order statistics for the sum of n scintillating signals of the form

$$Y(t) = \sum_{k=1}^{n} a_k \cos\left[K(t-t_k)^2 + \phi_k\right] \qquad \text{for} \quad 0 \leqslant t \leqslant T \tag{19}$$

cannot be derived. However, several important properties for the sum of many scintillating signals can readily be obtained. For example using Eq. (13), the mean value of Eq. (19) is immediately obtained

$$\text{Mean}\{Y\} \sim \frac{1}{4T}\left(\frac{\pi}{K}\right)^{1/2} \sum_{k=1}^{n} a_k \cos\left(\frac{\pi}{4} + \phi_k\right). \tag{20}$$

Similarly an explicit expression for the variance of Eq. (19) can be obtained, this is

$$\sigma^2(\tau) \sim \frac{1}{2}\sum_{k=1}^{n} a_k^2 + \sum_{\text{all pairs}} a_k a_l\, \delta(t_k - t_l) + \frac{1}{32T}\left(\frac{2\pi}{K}\right)^{1/2} \sum_{k,l=1}^{n} a_k a_l \left\{\cos\left(\frac{\pi}{4} + \phi_{kl}\right)\right.$$

$$\left. - \frac{1}{T}\left(\frac{2\pi}{K}\right)^{1/2} \cos\left(\frac{\pi}{4} + \phi_k\right)\cos\left(\frac{\pi}{4} + \phi_l\right)\right\} \tag{21}$$

where δ is the Kronecker delta function and $\phi_{kl} = (K/2)(t_k - t_l + \tau)^2 + (\phi_k + \phi_l)$.

It is not difficult to arrive at the result that the worst clutter case (greatest probability of false alarm for a given threshold level) will occur when all the point-scatterers are lumped together and add constructively. For this case the variance takes the form

$$\sigma^2 \sim \frac{1}{2}\left(\sum_{k=1}^{n} a_k\right)^2 + O\left(\frac{1}{T\sqrt{K}}\right), \tag{22}$$

and the first-order statistics are those for a single scintillating signal of amplitude equal to the sum of the component amplitudes.

Another interesting case is that in which the components' scintillating signals can be considered mutually independent. In this case the variance is of the form

$$\sigma^2 \sim \frac{1}{2}\sum_{k=1}^{n} a_k^2 + O\left(\frac{1}{T\sqrt{K}}\right), \tag{23}$$

in which the first sum is the variance of n sine waves of irrational periods and of amplitude identical to those of the scintillating signals.

Although the first-order statistics of the sum of several scintillating signals cannot be obtained explicitly, they can be derived very conveniently by computer simulation. In Fig. 5 the computer simulation has been performed for the case of two-scintillating signals. The amplitude of one component is kept constant, while the amplitude of the other component is varied from 0 to 1, in steps of 0.2.

Since the mean value of scintillating signals is nonzero, the distribution of the sum of many scintillating signals should converge to the Gaussian distribution according to Eq. (18) and the number of components is the number of independent subsets. Here, we will not

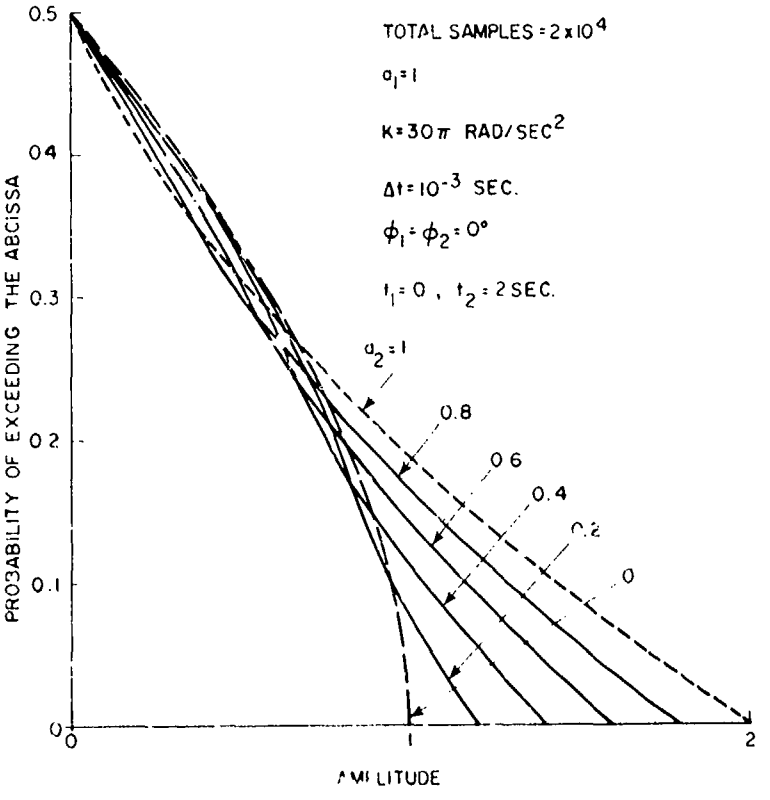

Fig. 5—The distribution function for the sum of two-scintillating signals

attempt to define what we mean by independent subsets in terms of the scintillating signals. Our aim is only to emphasize the slower rate of convergence of the distribution of the sum of scintillating signals toward the Gaussian distribution. This is illustrated in Fig. 6 in which the distribution of a number of scintillating signals, for point-scatterers of equal amplitude in an array configuration, was obtained by computer simulation for different numbers of scintillating signals. The limiting distributions are the distribution for one scintillating signal and the Gaussian distribution. Surprisingly enough the distribution for the sum of a large number of scintillating signals has long tails, similar to the lognormal distribution. Thus, seemingly we have discovered a new mechanism that yields lognormal clutter.

Based on the asymptotic properties of the first-order statistics of the sum of scintillating signals, the distribution of the return from a point-scatterer in a homogeneous Gaussian clutter may be approximated by the well-known statistical results for a sine wave in Gaussian noise (8-10). In Fig. 7, Rice results (9) have been used to represent the distribution of a point-scatterer in various amounts of Gaussian clutter.

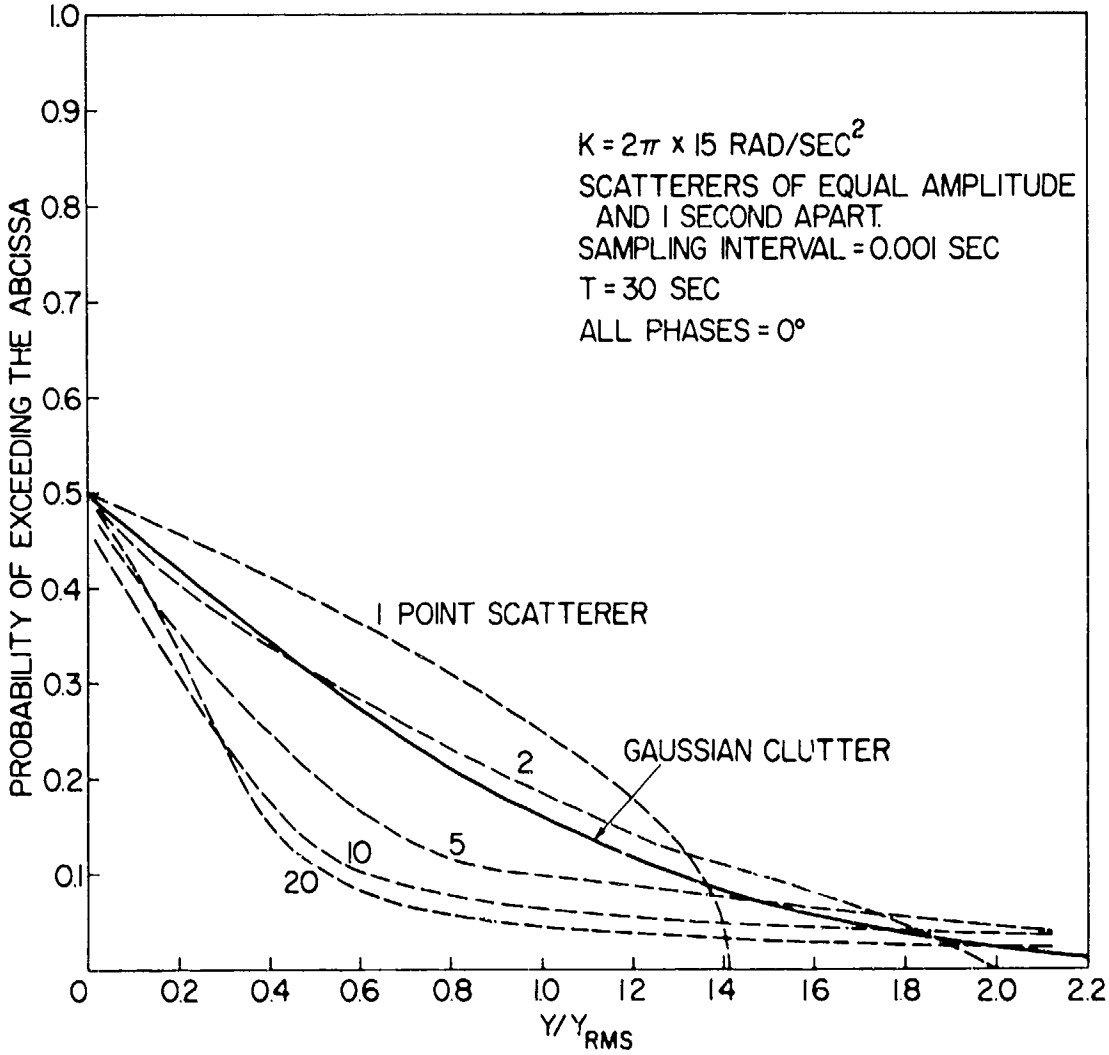

Fig. 6—The distribution function of the sum of several scintillating signals

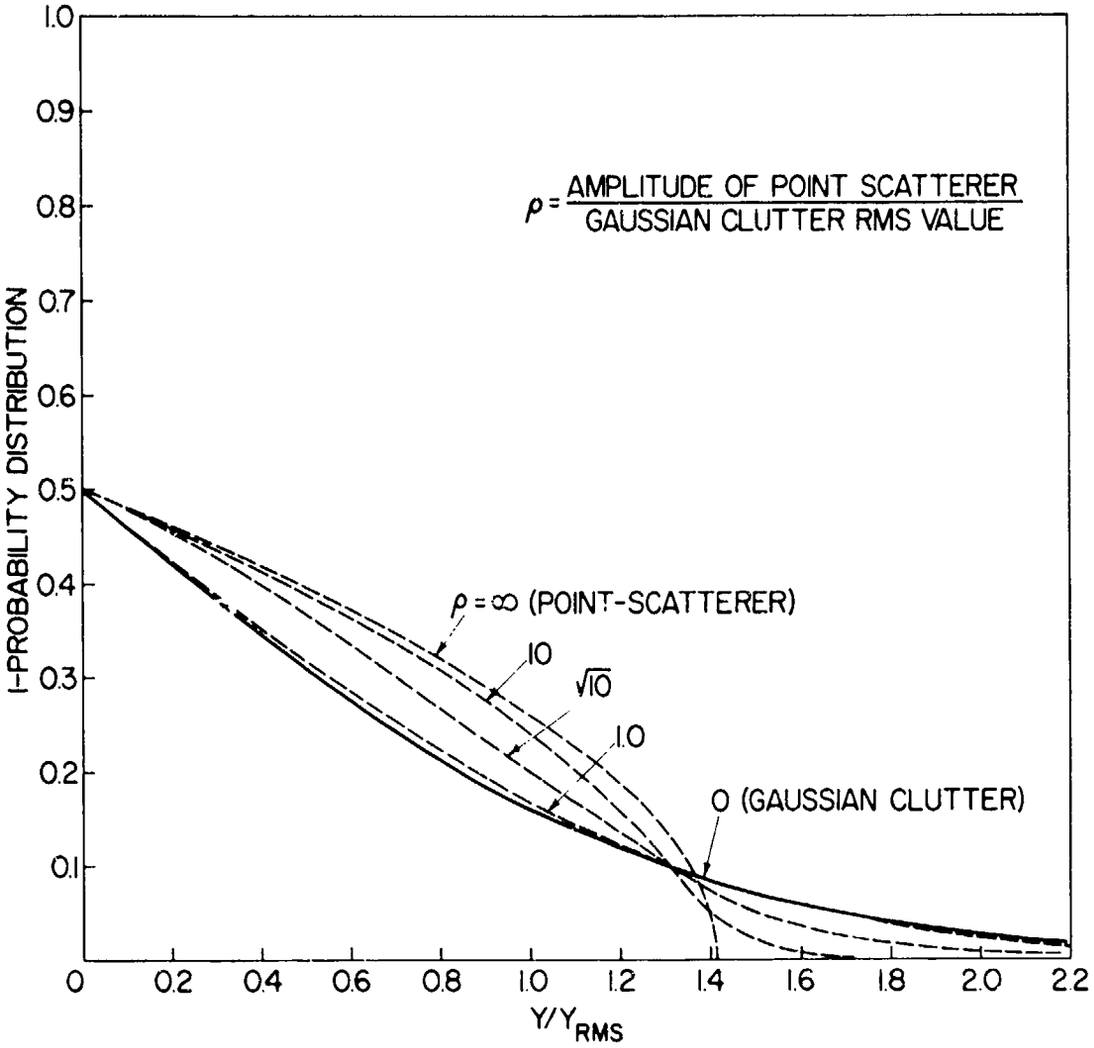

Fig. 7—The distribution of a point-scatterer in Gaussian clutter

In terrain clutter measurements taken with the 4FR system over Phoenix, Arizona, on Oct. 7, 1966, the lognormal and specular nature of clutter was quite evident. In Fig. 8 a couple of these interesting distributions of the complete signal are displayed. (The output of the amplitude and phase channels of the 4FR system have been combined to form $E \cos \phi$; E is the envelope of the clutter and ϕ is the instantaneous phase.) The distribution for P-Band exhibits the long tail typical of lognormal clutter, quite similar to those given in Fig. 6 and obtained by computer simulation. The distribution for C-Band may be a composite, produced by a couple of strong point-scatterers in a background of weaker Gaussian clutter.

STATISTICS OF THE ENVELOPE

In many applications one is interested mainly in the statistics of the envelope $E(t)$ of terrain—in particular in incoherent radars. The envelope of Eq. (3) is given by

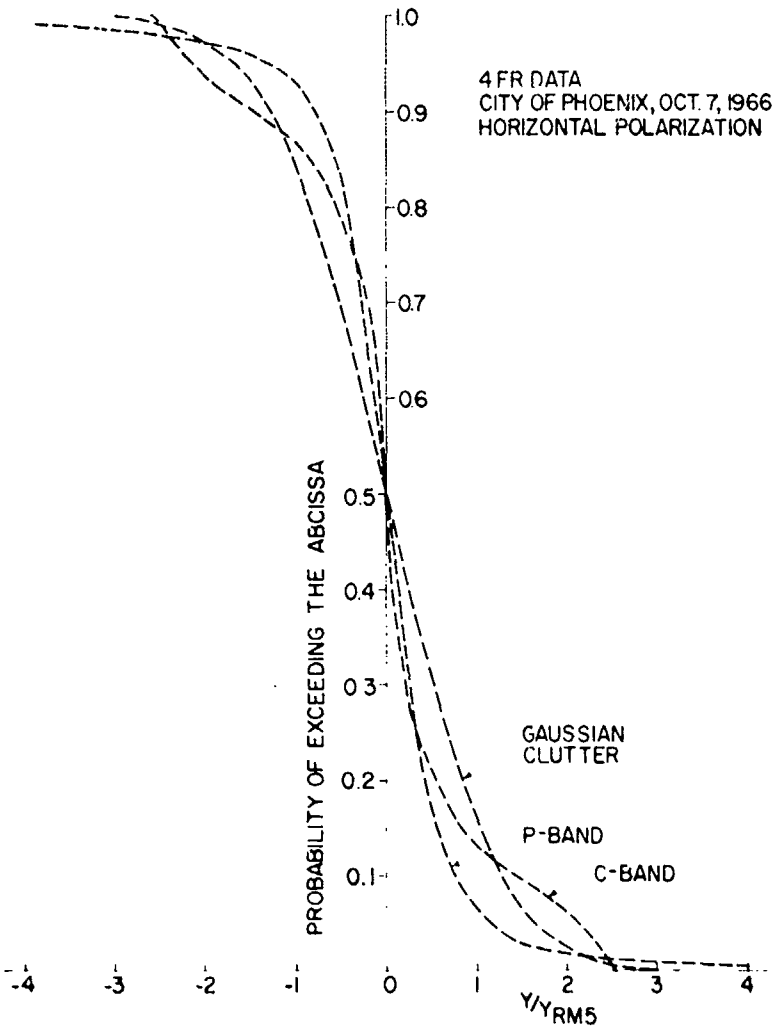

Fig. 8—Cumulative distributions obtained with the 4FR system over Phoenix, Arizona, in 1966 which support the specular nature of terrain clutter

$$E(t) = \left\{ \left(\sum_{k=1}^{n} a_k \cos\left[\phi_k + K(t - t_k)^2\right] \right)^2 + \left(\sum_{k=1}^{n} a_k \sin\left[\phi_k + K(t - t_k)^2\right] \right)^2 \right\}^{1/2} \tag{24}$$

or

$$E(t) = \left\{ \sum_{k=1}^{n} a_k^2 + 2 \sum_{\substack{\text{all pairs} \\ k \neq l}} a_k a_l \cos\left[(\phi_k - \phi_l) + K(t_k - t_l)^2 - 2K(t_k - t_l)t\right] \right\}^{1/2}. \tag{25}$$

Interestingly enough the mean value of E^2 is given by

$$\text{Mean}\left\{E^2\right\} = \sum_{k=1}^{n} a_k^2 \qquad \text{for} \quad \phi_k \neq \phi_l\,, \tag{26}$$

which also is related to the mean power of the incoherent clutter.

Thus since Eq (26) also represents the mean value for the superposition of sine waves of amplitude similar to the scintillating signals, one would suspect that the distribution of the envelope of terrain clutter may converge faster to the Rayleigh distribution than the distribution of the complete signal (amplitude and phase) will converge to the Gaussian distribution. Recalling the results for a sine wave in Gaussian noise, a point-scatterer in Gaussian clutter should have an envelope which is Rician distributed.

The convergence of the first-order statistics of the envelope of the sum of many random processes toward the Rayleigh distribution is reviewed in detail by Beckmann (11).

For example the envelope of the sum of n sinusoidal signals of irrational periods and amplitude a_k converge toward the Rayleigh distribution according to the expression

$$p(E) \sim \frac{E}{\sigma^2} e^{-E^2/2\sigma^2}\left\{1 - \frac{1}{64}\frac{\sum_{k=1}^{n} a_k^4}{\sigma^4}\left(8 - 8\xi^2 + \xi^4\right) + \ldots\right\}, \tag{27}$$

for the density and

$$P\left\{\frac{E}{\sigma\sqrt{2}} > R\right\} \sim e^{-R^2}\left\{1 - \frac{\sum_{k=1}^{n} a_k^4}{16\sigma^4}\left(R^4 - 2R^2\right) + \ldots\right\}, \tag{28}$$

for the distribution function, where

$$2\sigma^2 = \sum_{k=1}^{n} a_k^2$$

$$\xi = \frac{E}{\sigma}\,.$$

The more general question on the rate of convergence of the envelope of the sum of independent random processes, each distributed according to a different distribution, can be shown to converge to the Rayleigh distribution according to the expression

$$p(E) \sim \frac{2E}{M_2} e^{-E^2/M_2}\left\{1 + \frac{1}{4}\frac{\left(M_4 - 2M_2'\right)}{M_2^2}\left(2 - 4\xi^2 + \xi^4\right) + \ldots\right\}. \tag{29}$$

for the density with $\xi = E/M_2^{1/2}$ and

$$P\left\{\frac{E}{\sqrt{M_2}} > R\right\} \sim e^{-R^2}\left\{1 + \frac{1}{4}\frac{(M_4 - 2M_2')}{M_2^2}(R^4 - 2R^2) + \ldots\right\}, \qquad (30)$$

for the distribution function, where

$$M_2 = \sum_{k=1}^{n} m_{2k},$$

$$M_2' = \sum_{k=1}^{n} m_{2k}^2,$$

$$M_4 = \sum_{k=1}^{n} m_{4k},$$

and m_{2k} and m_{4k} are the second and fourth moments of the component random processes. Beckmann's expression (38) in Ref. 11 is incorrect; a quadratic term in the series for the distribution is missing. Compare with our (30).

INFERENCE OF THE STATISTICS OF TERRAIN CLUTTER

In this section, the statistics of terrain clutter as observed with the 4FR system is investigated. The 4FR system transmits at 428 MHz (UHF or P-Band), 1228 MHz (L-Band), 4455 MHz (C-Band) and at 8910 MHz (X-Band). An excellent description of the 4FR system can be found in Ref. 1. Since the amplitude channel is completely calibrated, these data will be used in the inference of the statistics of terrain clutter. The outputs of the amplitude channel are samples of radar cross section of terrain (in units of decibels) as a function of time and can be normalized by the area on the terrain illuminated by the radar.

The data used in this investigation were collected by the radar, in side looking operation, on Oct. 6, 1966, over Arizona and contain return from deserts, mountains, farmland, and local communities. Additional information on the measurements can be found in Ref. 12.

The cumulative distribution of the NRC of terrain is checked with the Kolmogorov-Smirnov test (13) against the exponential and the lognormal distributions. Finally, the first five central moments of the samples (in units of decibels) of the NRC of terrain are obtained. Clearly, if all the moments were known, the exact distribution of terrain clutter could be reconstructed.

It was decided, for obvious practical reasons of terrain identification, that the total number of samples used in each distribution and moment computation should not exceed the time in which the airplane takes to travel the distance equal to the azimuth antenna

beamwidth illumination of the terrain. Thus the total number of samples used in each distribution, or moments computation, is a function of airplane altitude, speed, antenna depression angle, and antenna azimuth beamwidth. The total number of samples used in each computation ranged from about 900 to 11,000.

The Distribution Function

The Kolmogorov-Smirnov test is a distribution-free type of statistical test used to test the hypothesis if the cumulative distribution obtained from a set of independent samples taken from a population belongs to a theorized distribution for the population. The number of independent samples for the terrain clutter data was determined by a standard run test (14) on groups of 1024 consecutive samples. The cumulative distribution of terrain clutter (between the 0 and the 100 percentile) are then tested against the exponential and the lognormal distributions. In the comparison with the exponential, the mean value of the theorized distribution was adjusted for the smallest maximum deviation between the distributions. In the comparison with the lognormal distribution, the variance and the median of the theorized distribution were taken to be that of the sample.

The Kolmogorov-Smirnov test, at the 99% level of significance (i.e., the cumulative distribution is accepted as belonging to the theoretical distribution if the maximum deviation is less than or equal to the critical value as given by Ref. 13) shows that in general the NRC of terrain is not exponentially distributed (with Rayleigh envelope) nor lognormal distributed. However, specific sections of data may be found to be exponentially distributed and on a few occasions, for small independent samples sizes, the data may be found to be lognormal.

For example in Figs. 9 and 10, the data is very likely to be exponentially distributed, while in Figs. 11 through 15 the data are neither exponential or lognormal. As a matter of fact, cumulative distributions which have long tails, typical of lognormal distributions, fail the Kolmogorov-Smirnov test in comparison with a lognormal distribution between the 0 and the 100 percentiles. Thus, strictly speaking terrain clutter may never be lognormal distributed and only the tails of the distribution may be approximable by this distribution.

The Central Moments

For purposes of identifying the statistics of terrain clutter in a more definite manner, the first five central moments of the NRC of terrain clutter (in units of decibels) will be derived from the amplitude samples of the 4FR system.

The central moments $\mu_1, \mu_2, \ldots, \mu_n$ of a random variable which is exponentially or lognormal distributed are well known and can be used for comparison. The central moments for the logarithm of a random variable which is exponentially distributed are related to the Poligamma function (15). The Poligamma function $\Psi^{(\nu-1)}(x)$ is defined as

$$\Psi^{(\nu-1)}(x) = \frac{d^{\nu}}{dx^{\nu}} \left[\ln \Gamma(x+1) \right] , \tag{31}$$

where $\Gamma(x+1)$ is the Gamma function. The central moments of the natural logarithm of a random variable which is exponentially distributed are constants given by

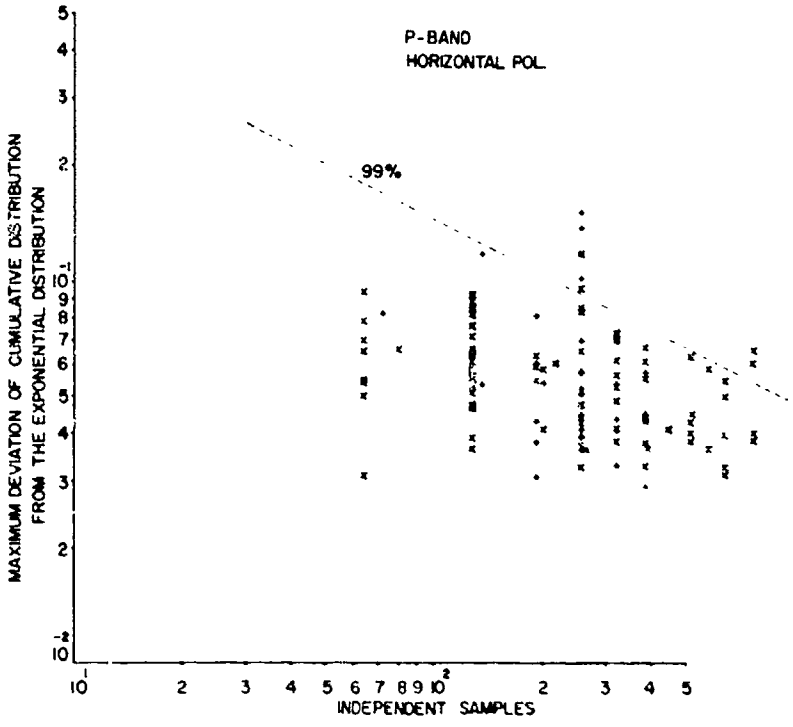

Fig. 9—Maximum deviation of the cumulative distribution of terrain clutter from the exponential distribution (with Rayleigh envelope)

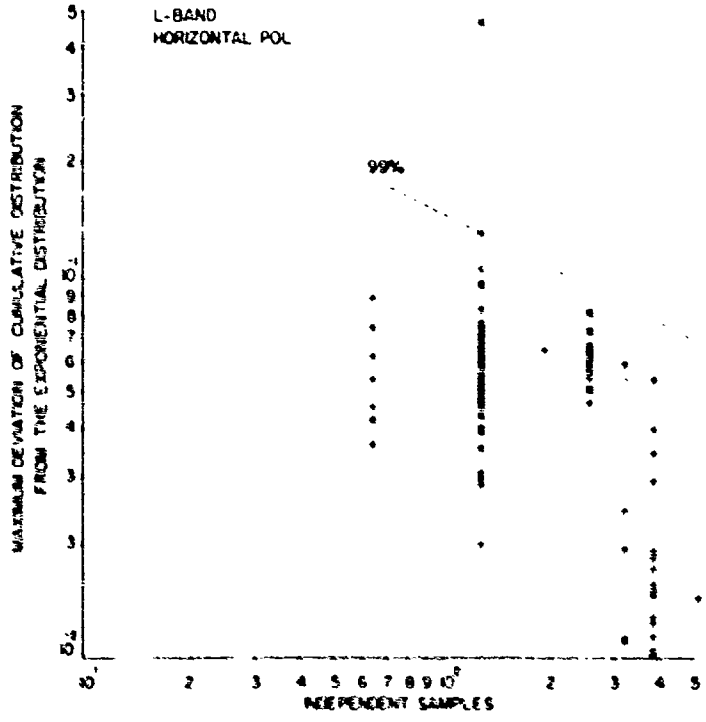

Fig. 10—Maximum deviation of the cumulative distribution of terrain clutter from the exponential distribution (with Rayleigh envelope)

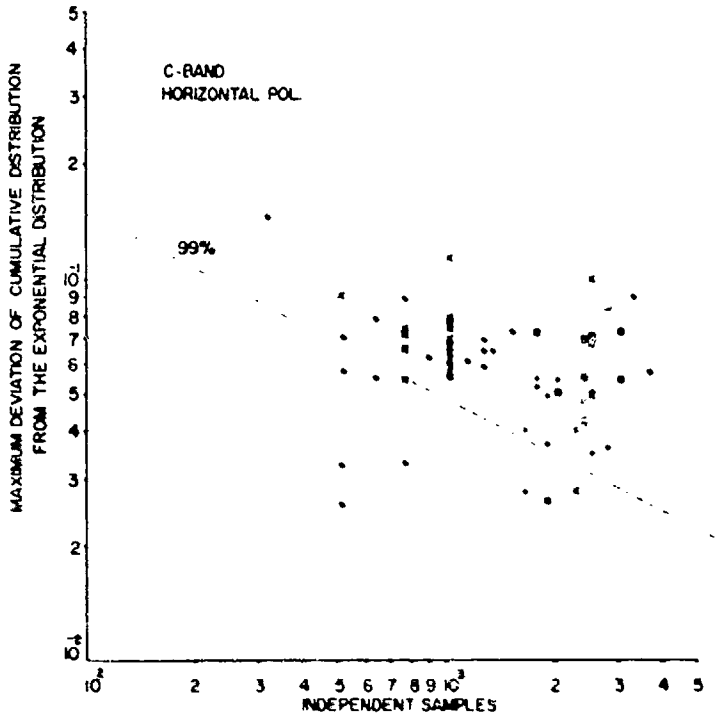

Fig. 11—Maximum deviation of the cumulative distribution of terrain clutter from the exponential distribution (with Rayleigh envelope)

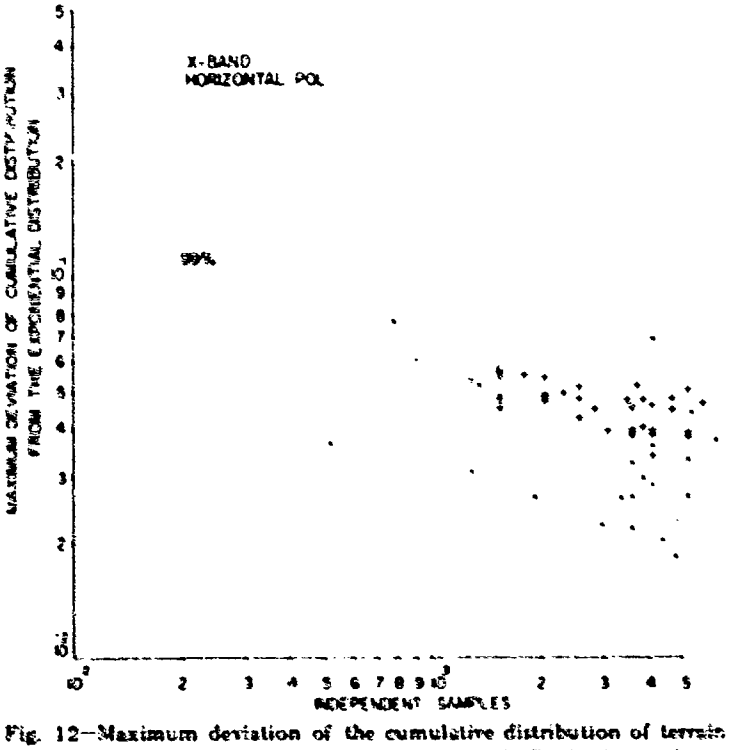

Fig. 12—Maximum deviation of the cumulative distribution of terrain clutter from the exponential distribution (with Rayleigh envelope)

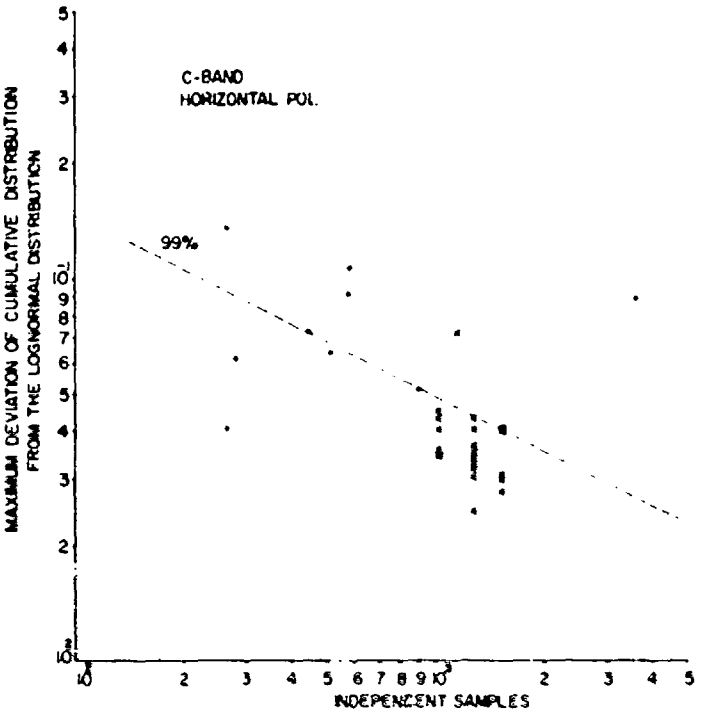

Fig. 13—Maximum deviation of the cumulative distribution of terrain clutter from the lognormal distribution

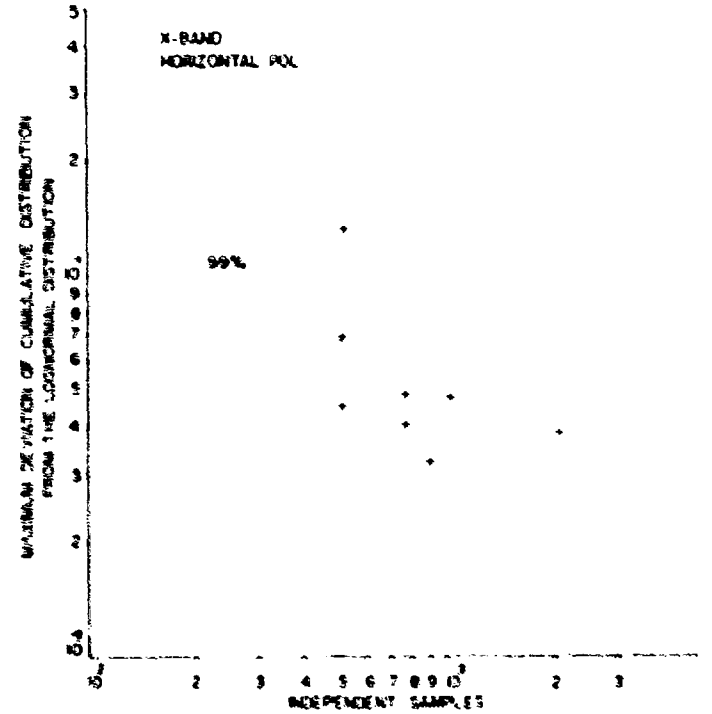

Fig. 14—Maximum deviation of the cumulative distribution of terrain clutter from the lognormal distribution

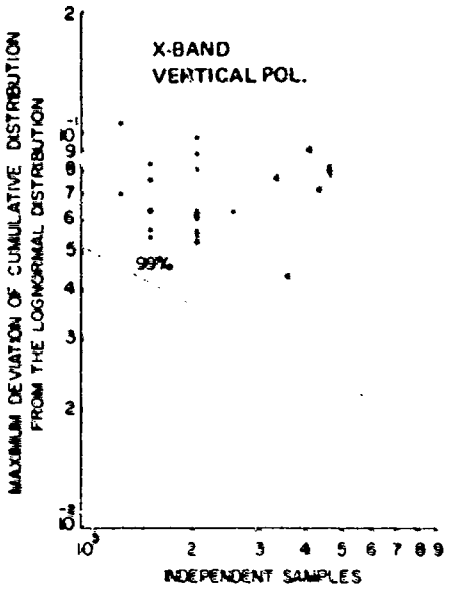

Fig. 15—Maximum deviation of the cumulative distribution of terrain clutter from the lognormal distribution

$$\begin{aligned} \mu_2 &= \Psi'(0) = 1.64493 \\ \mu_3 &= \Psi''(0) = -2.40411 \\ \mu_4 &= \Psi'''(0) = 6.49393 \\ \mu_5 &= \Psi^{IV}(0) = -24.88627 \end{aligned} \tag{32}$$

and $\Psi(0) = 0.5772157$ is the difference between the natural logarithm of the mean value of the exponentially distributed random variable and the mean value of the natural logarithm of the random variable. The numerical values of the Poligamma function were obtained from Davis (16).

Similarly, the central moments of a random variable (exponentially distributed in amplitude), in decibel units are related to Eq. (32) by a constant; that is,

$$\begin{aligned} \mu_2 &= c^2\Psi'(0) \\ \mu_3 &= c^3\Psi''(0) \\ \mu_4 &= c^4\Psi'''(0) \\ \mu_5 &= c^5\Psi^{IV}(0) \end{aligned} \tag{33}$$

where $c = 10 \log_{10} e$ with $e = 2.7182818$, and the difference between the median and the mean value of the random variable in decibels is approximately 0.91.

The central moments of the logarithm of a random variable which normally is log-normal distributed are those of the Gaussian distribution

$$\mu_n = \mu_2^{n/2} \prod_{k=1}^{n/2} (2k-1), \tag{34}$$

where $n \geq 2$ and is even. If n is odd, $\mu_n = 0$.

In Figs. 16-55, the result of computing the central moments of terrain clutter for the four frequencies and both polarizations are shown. In these plots the corresponding values for the central moments for the exponential and the lognormal distribution are shown for comparison. Obviously, these results show that terrain clutter in general is neither exponential nor lognormal distributed, thus supporting the results of the Kolmogorov-Smirnov test on the cumulative distribution.

One obvious conclusion is that the type of terrain is principally reflected in the mean value of the clutter. In comparison with the previous empirical results obtained for sea clutter (17), now we find a greater spread in all the moments.

RESULTS AND CONCLUSIONS

In the first part of this investigation the point-scatterer formulation for the statistics of terrain clutter was developed. Although the model is quite general, specific results are given only for the case of a side-looking radar. We have shown that many of the statistical properties of terrain clutter can be derived with this formulation. An important result of this investigation is the relatively slow rate of convergence of the statistics for the sum of several scintillating signals toward the Gaussian distribution as the number of components increases. This happens because the mean value of a scintillating signal in general is nonzero.

The limiting distributions of terrain clutter are shown to be the Gaussian distribution, that obtained over homogeneous terrains such as deserts and farmland for example, and the distribution of a scintillating signal produced by a point-scatterer. Terrain clutter which has a distribution with long tails, typical of lognormal distributions, should be encountered over urban areas and over mountainous terrain. Figure 8 shows selected distributions of terrain clutter obtained with the 4FR system which have interesting features tending to support the point-scatterer formulation for the statistics of terrain clutter.

The empirical investigation of the statistics of the NRC of terrain, in decibel units, in general has neither exponential (of Rayleigh envelope) nor lognormal distribution. However, terrain clutter data from homogeneous terrains are very likely to be exponentially distributed (with Rayleigh envelope).

Strictly speaking, terrain clutter is never lognormal distributed between the 0 and 100 percentiles. However, in many instances the distribution of terrain has long tails typical

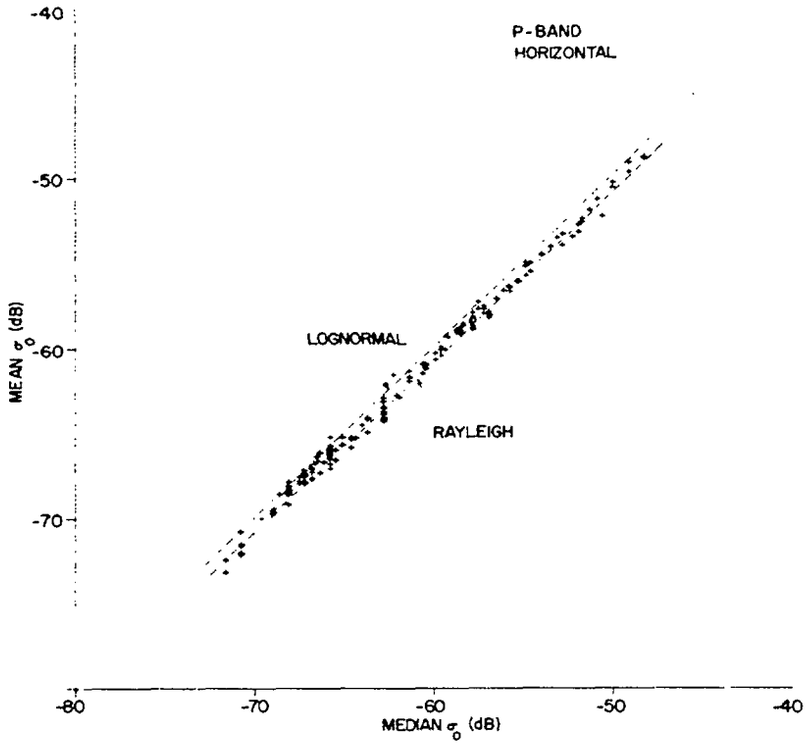

Fig. 16—The mean value vs the median value of the normalized radar cross section of terrain clutter (in decibel units)

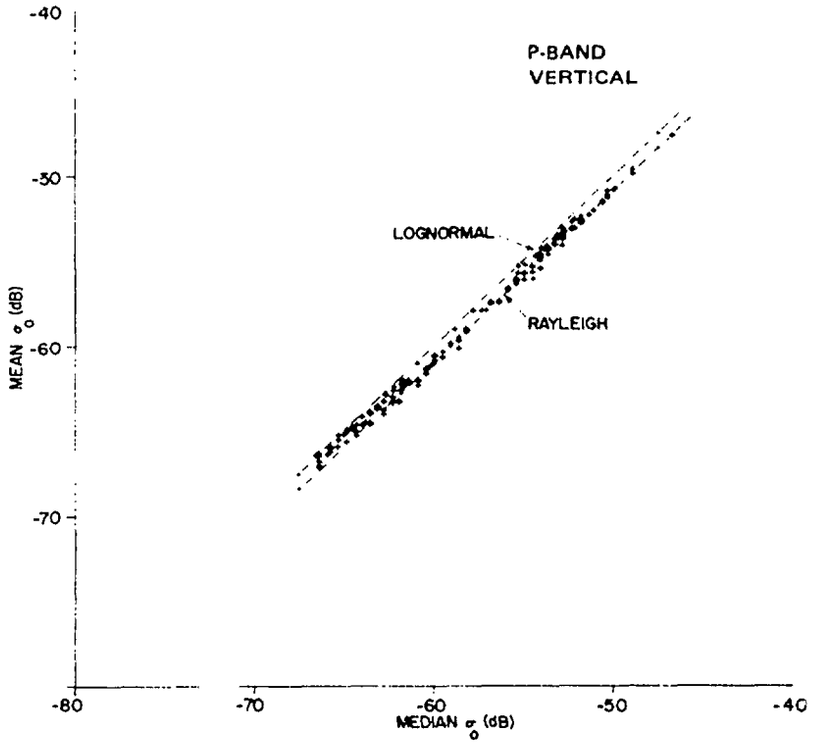

Fig. 17—The mean value vs the median value of the normalized radar cross section of terrain clutter (in decibel units)

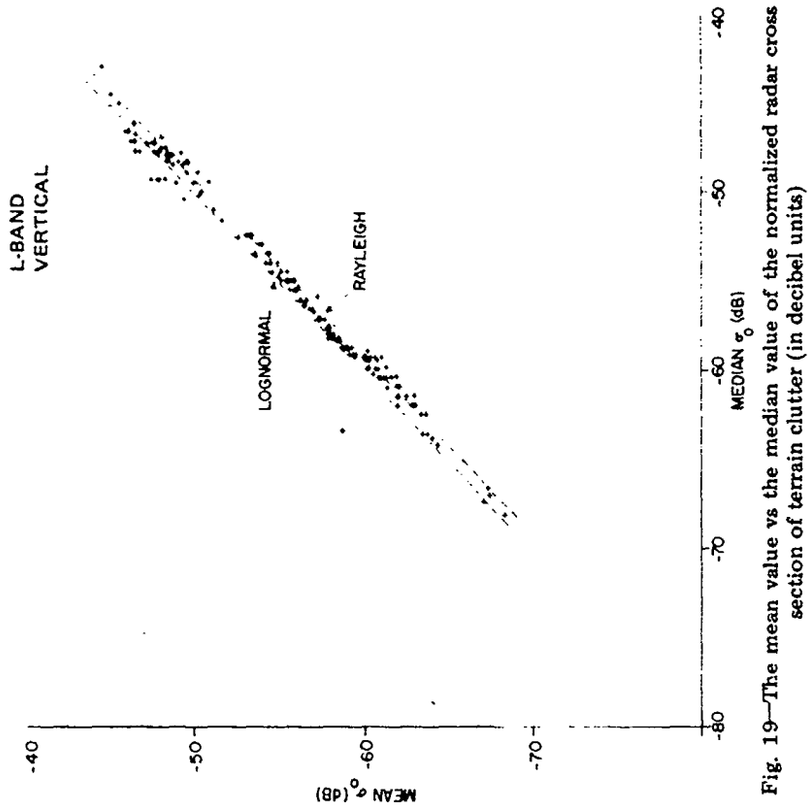

Fig. 19—The mean value vs the median value of the normalized radar cross section of terrain clutter (in decibel units)

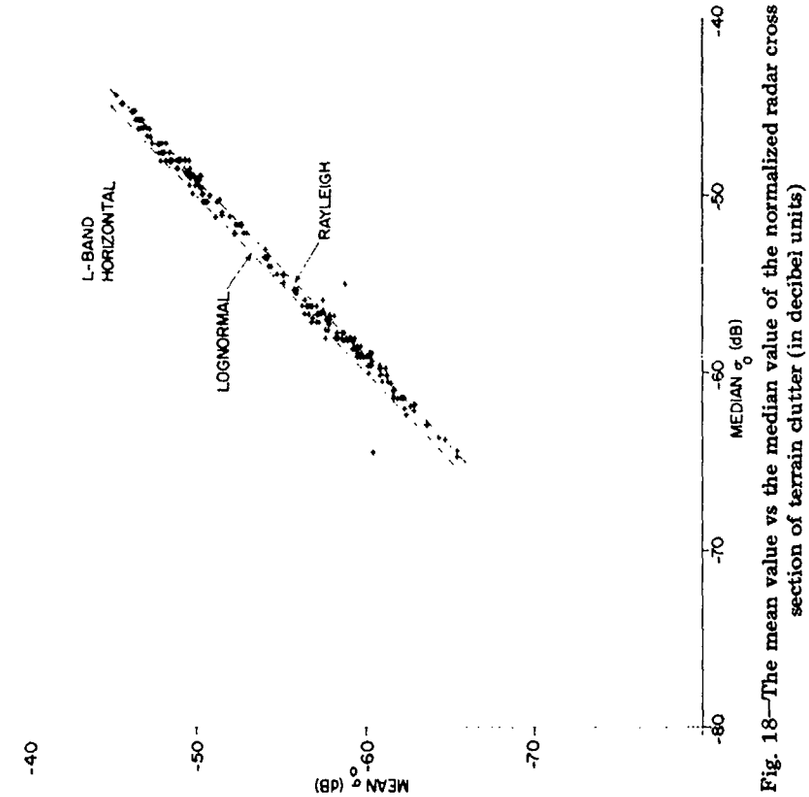

Fig. 18—The mean value vs the median value of the normalized radar cross section of terrain clutter (in decibel units)

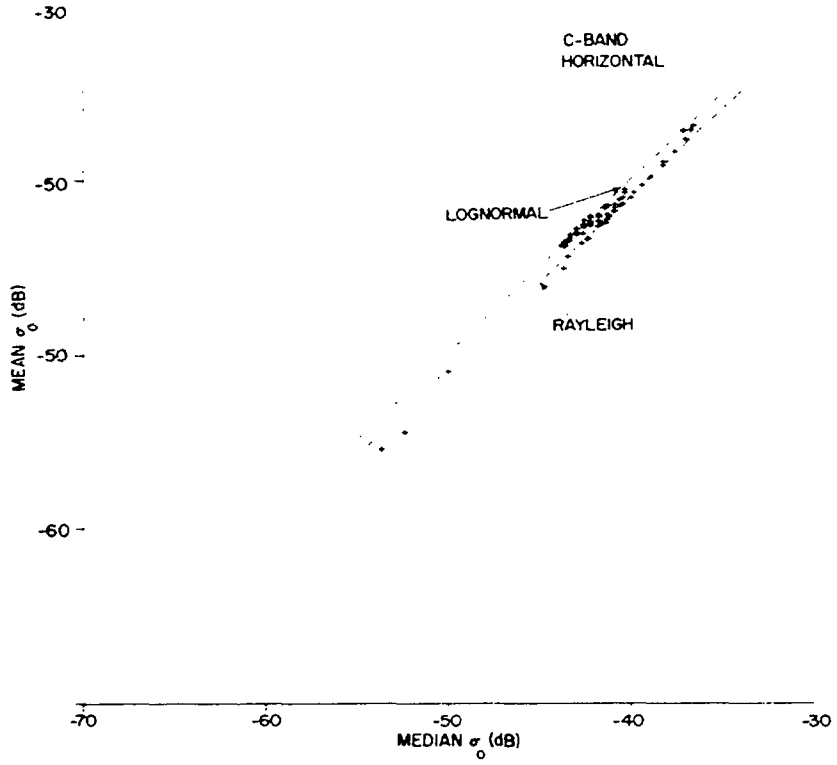

Fig. 20—The mean value vs the median value of the normalized radar cross section of terrain clutter (in decibel units)

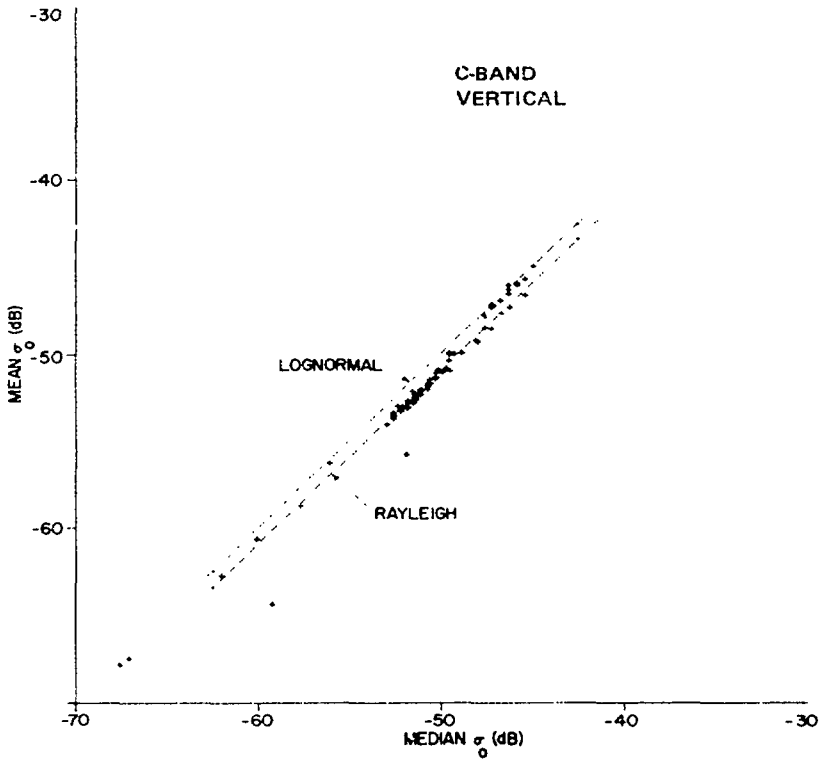

Fig. 21—The mean value vs the median value of the normalized radar cross section of terrain clutter (in decibel units)

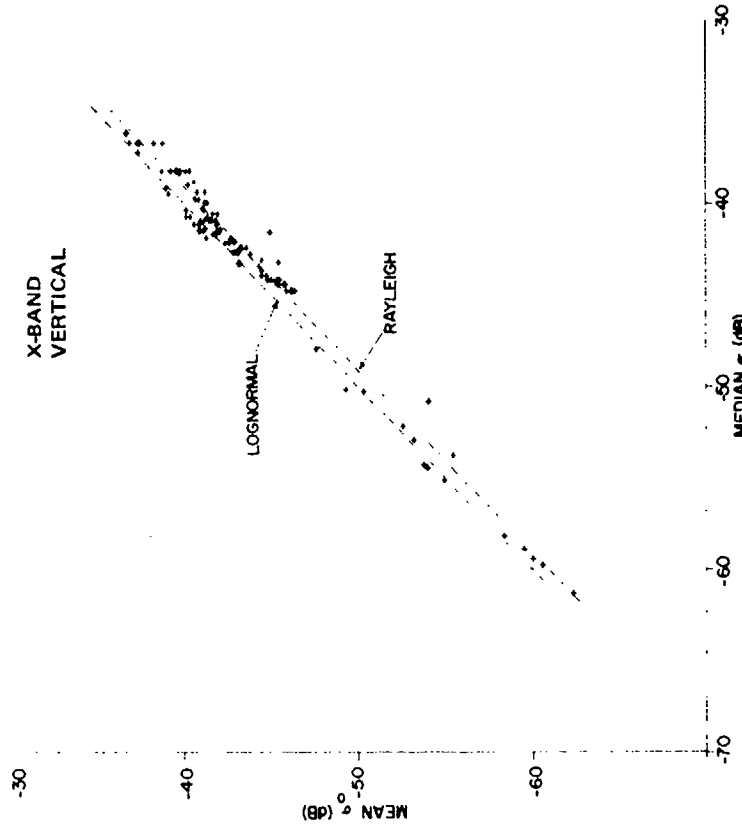

Fig. 23—The mean value vs the median value of the normalized radar cross section of terrain clutter (in decibel units)

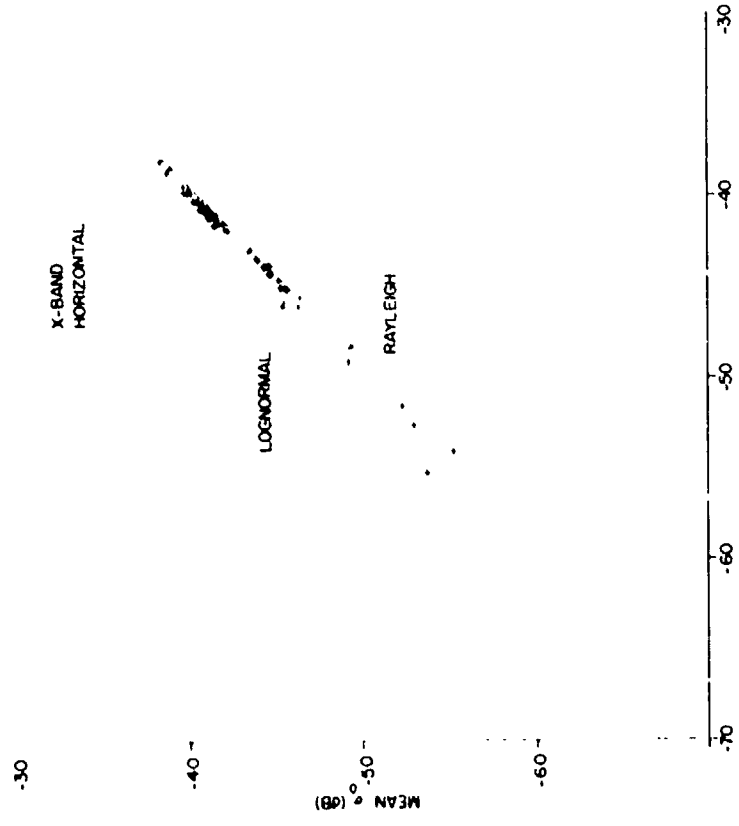

Fig. 22—The mean value vs the median value of the normalized radar cross section of terrain clutter (in decibel units)

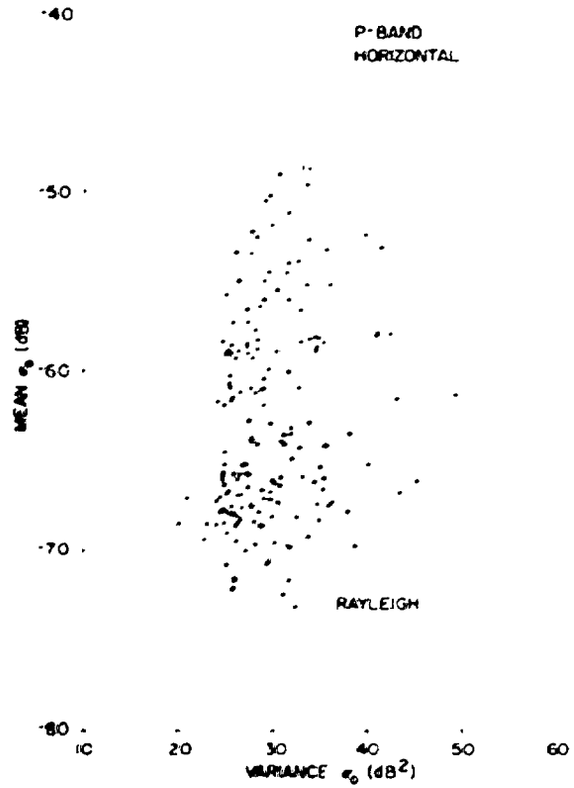

Fig. 24—The mean value vs the variance of the normalized radar cross section of terrain clutter (in decibel units)

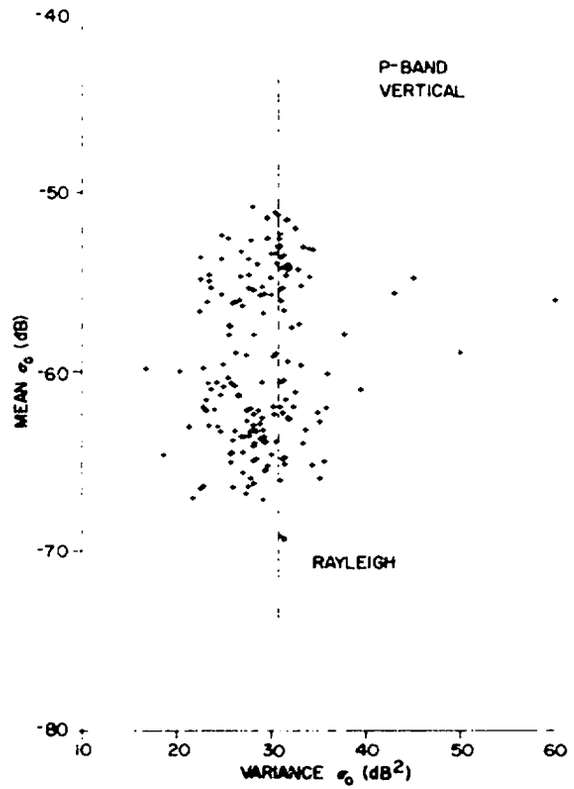

Fig. 25—The mean value vs the variance of the normalized radar cross section of terrain clutter (in decibel units)

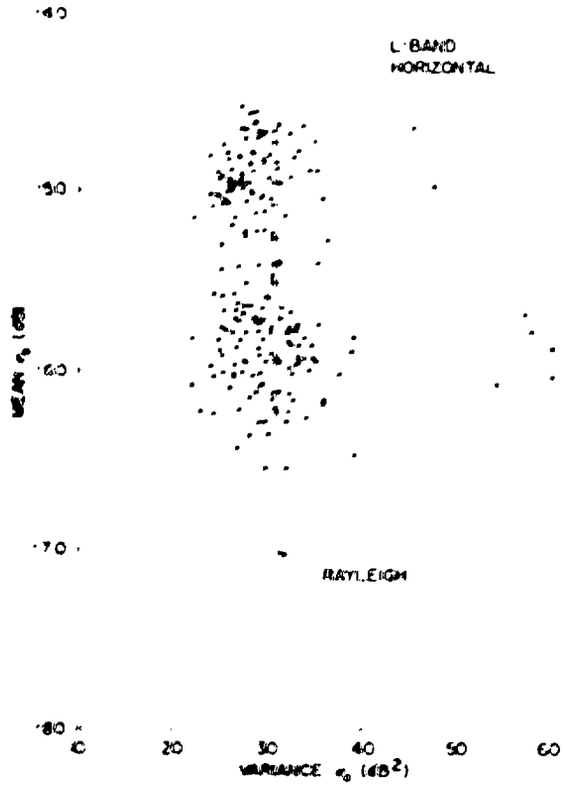

Fig. 26—The mean value vs the variance of the normalized radar cross section of terrain clutter (in decibel units)

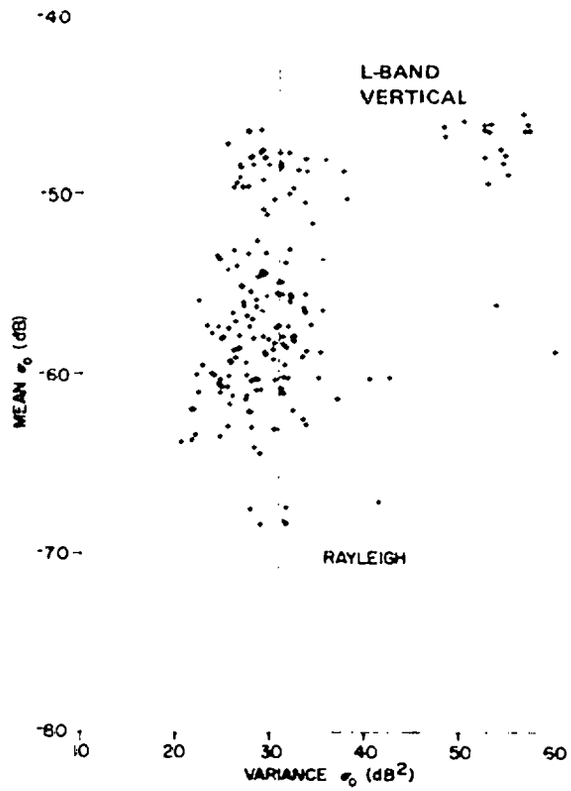

Fig. 27—The mean value vs the variance of the normalized radar cross section of terrain clutter (in decibel units)

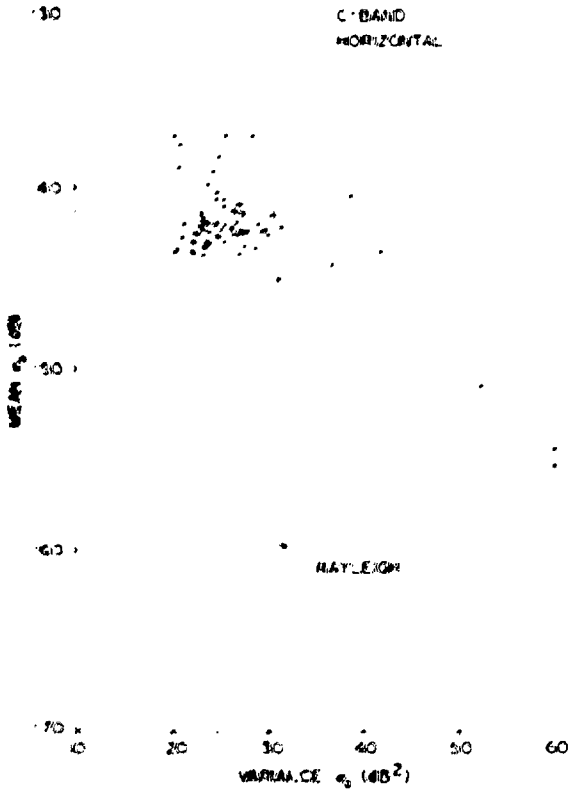

Fig. 28—The mean value vs the variance of the normalized radar cross section of terrain clutter (in decibel units)

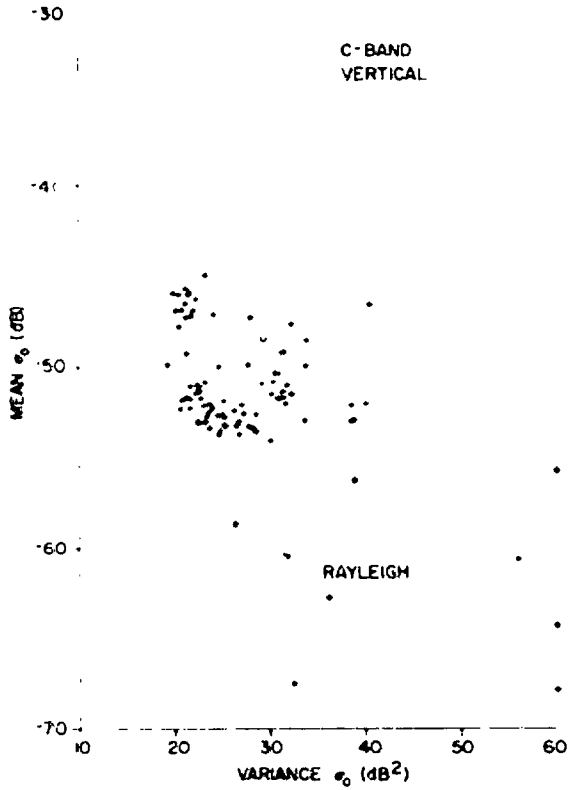

Fig. 29—The mean value vs the variance of the normalized radar cross section of terrain clutter (in decibel units)

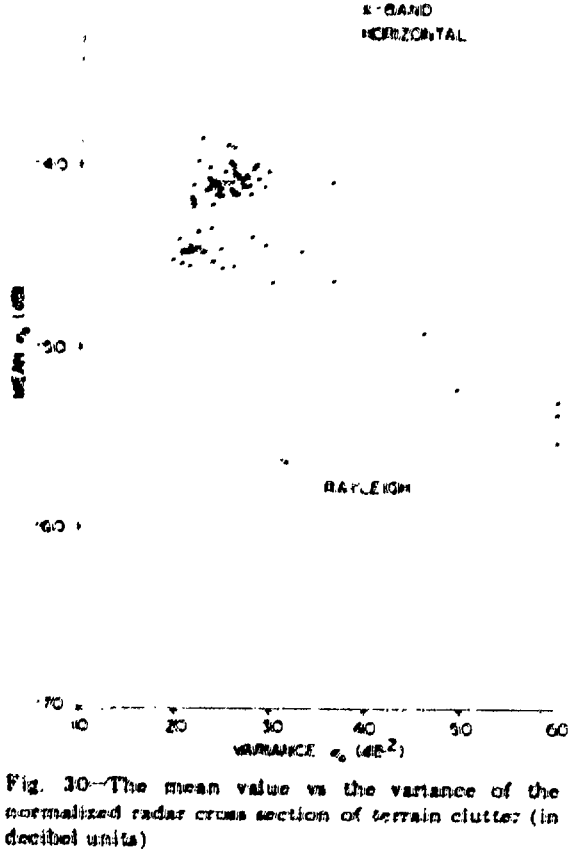

Fig. 30—The mean value vs the variance of the normalized radar cross section of terrain clutter (in decibel units)

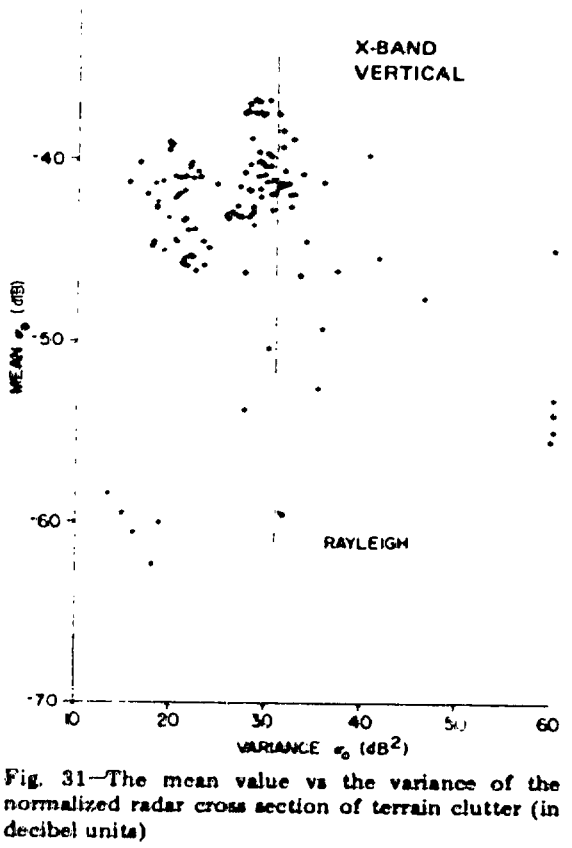

Fig. 31—The mean value vs the variance of the normalized radar cross section of terrain clutter (in decibel units)

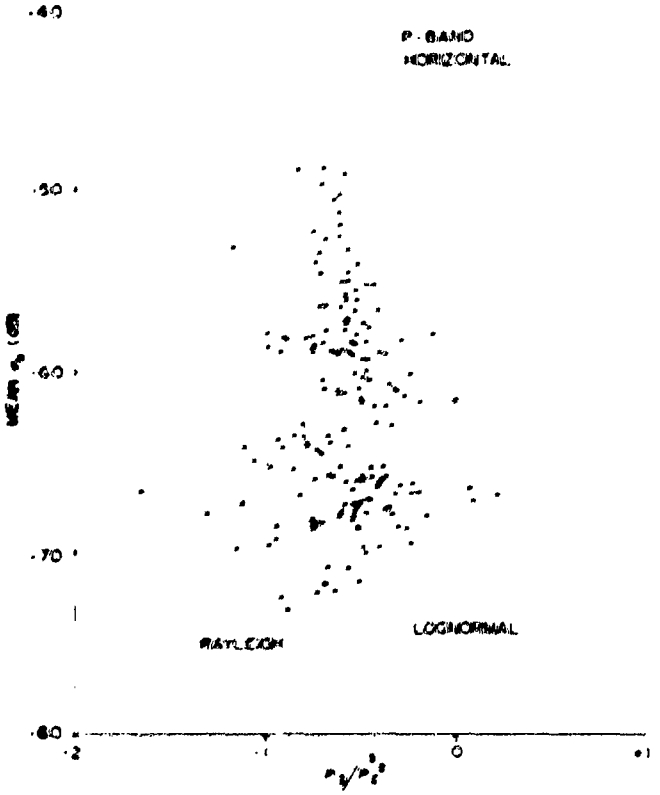

Fig. 32—The mean value vs $\mu_3/\mu_2^{3/2}$ of the normalized radar cross section of terrain clutter (in decibel units)

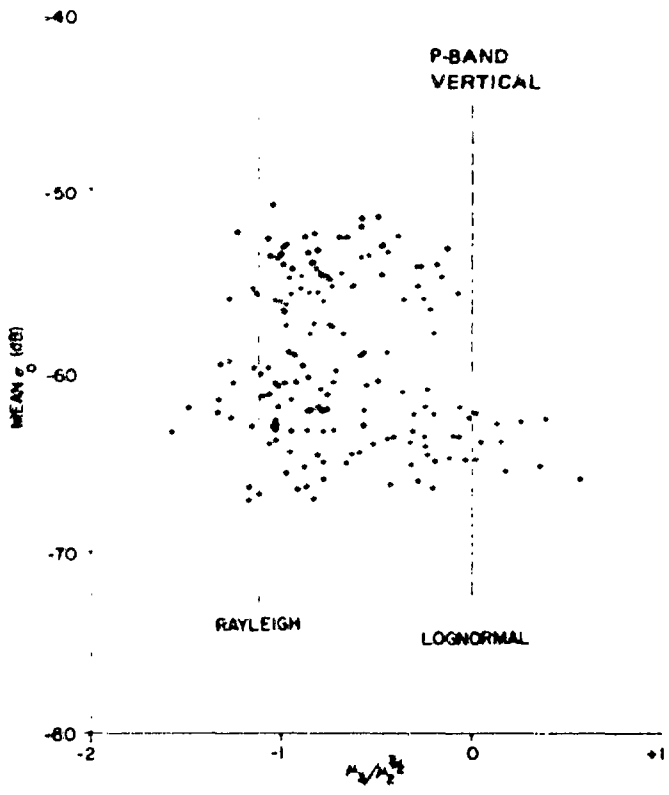

Fig. 33—The mean values vs $\mu_3/\mu_2^{3/2}$ of the normalized radar cross section of terrain clutter (in decibel units)

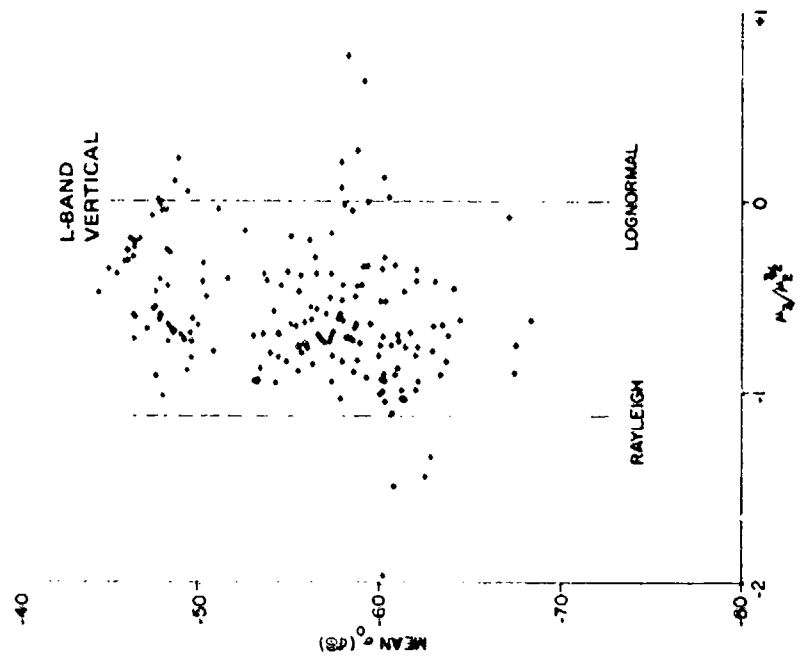

Fig. 35—The mean value vs $\mu_3/\mu_2^{3/2}$ of the normalized radar cross section of terrain clutter (in decibel units)

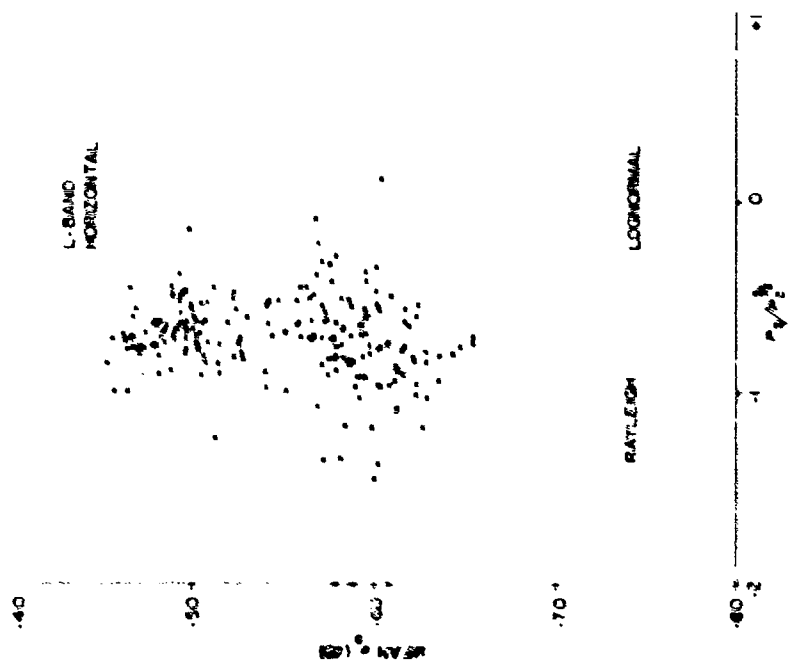

Fig. 34—The mean value vs $\mu_3/\mu_2^{3/2}$ of the normalized radar cross section of terrain clutter (in decibel units)

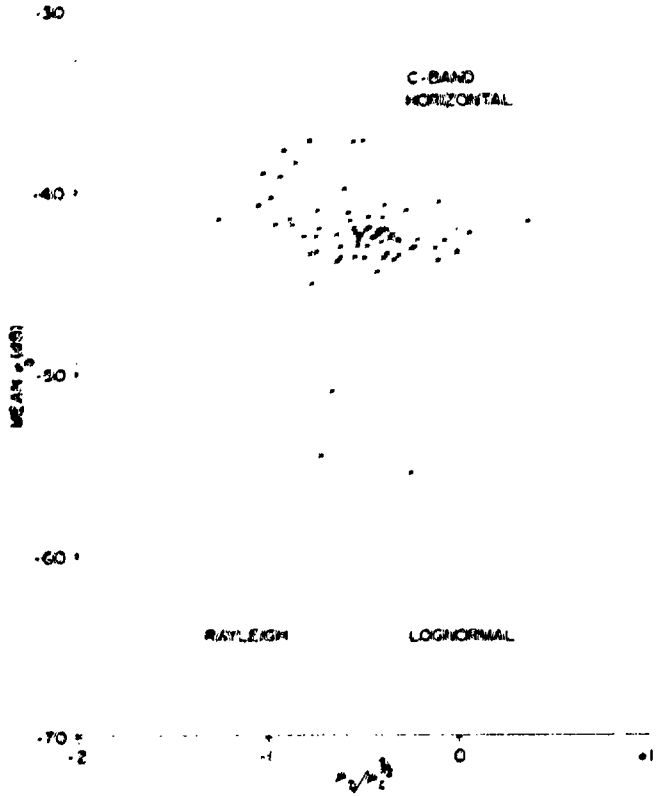

Fig. 36—The mean value vs $\mu_3/\mu_2^{3/2}$ of the normalized radar cross section of terrain clutter (in decibel units)

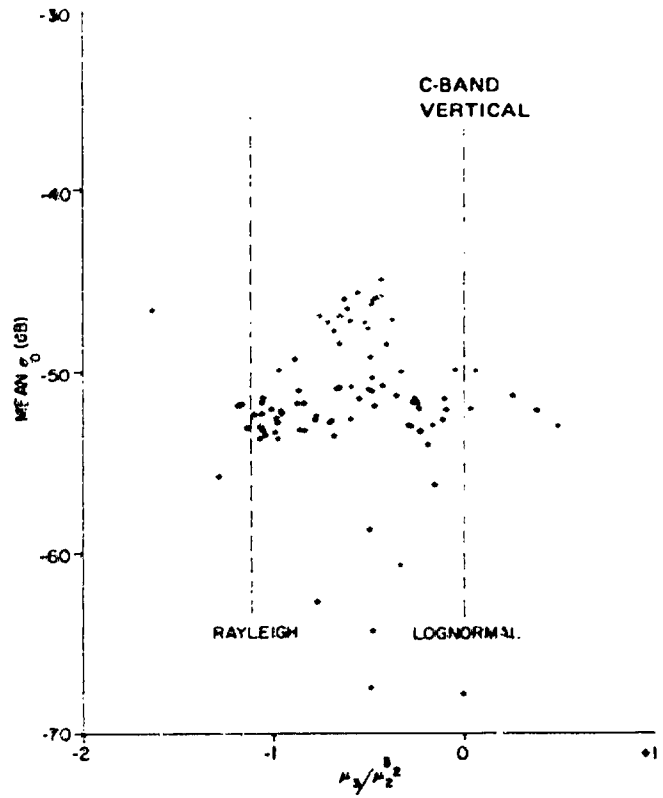

Fig. 37—The mean value vs $\mu_3/\mu_2^{3/2}$ of the normalized radar cross section of terrain clutter (in decibel units)

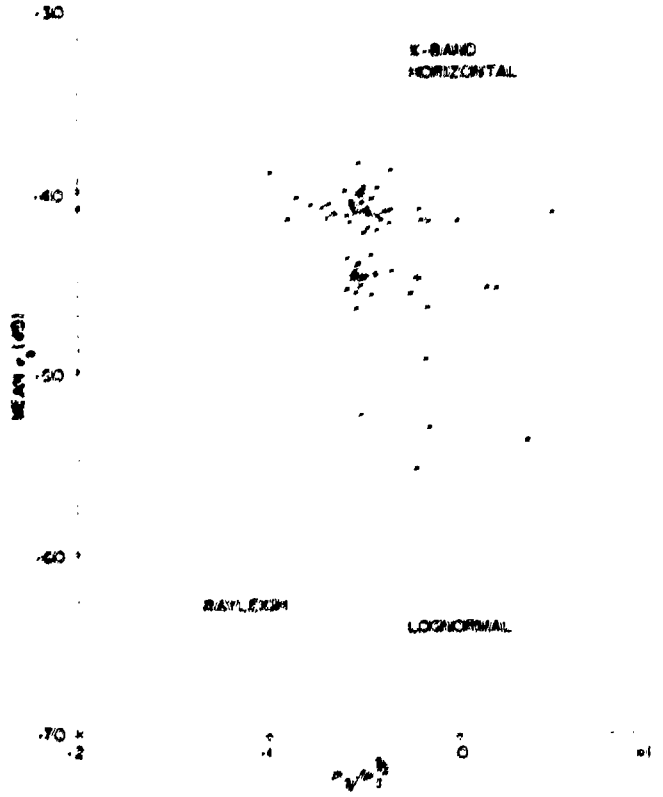

Fig. 38—The mean value vs $\mu_3/\mu_2^{3/2}$ of the normalized radar cross section of terrain clutter (in decibel units)

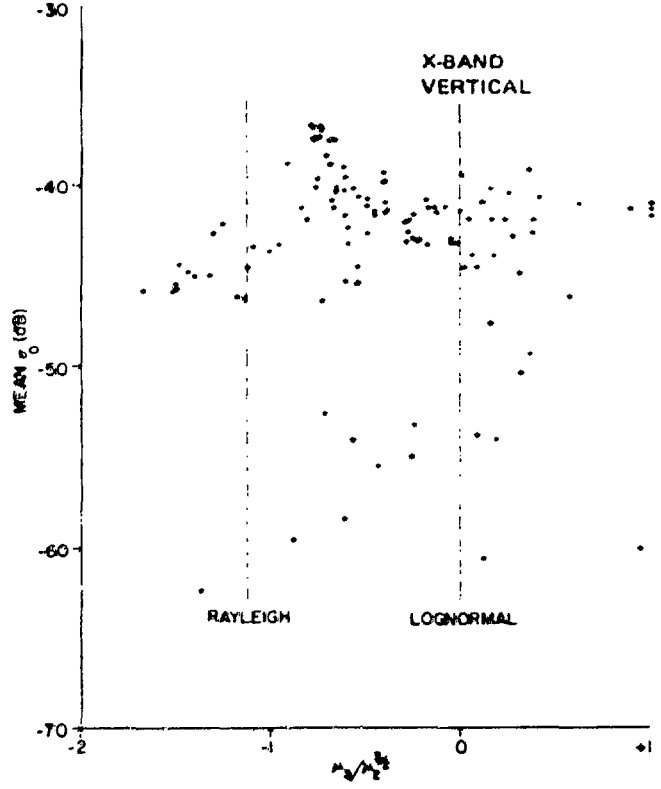

Fig. 39—The mean value vs $\mu_3/\mu_2^{3/2}$ of the normalized radar cross section of terrain clutter (in decibel units)

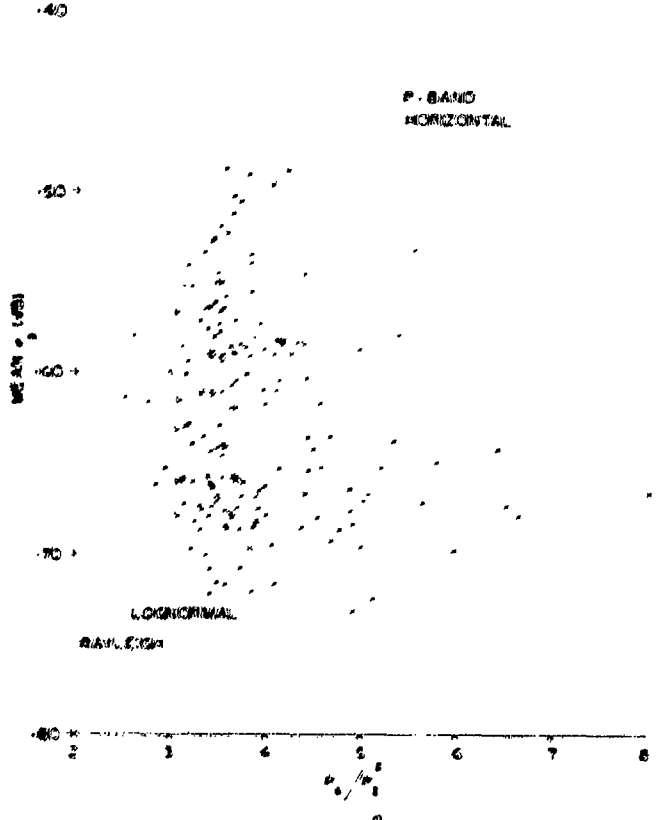

Fig. 40—The mean value vs μ_4/μ_2^2 of the normalized radar cross section of terrain clutter (in decibel units)

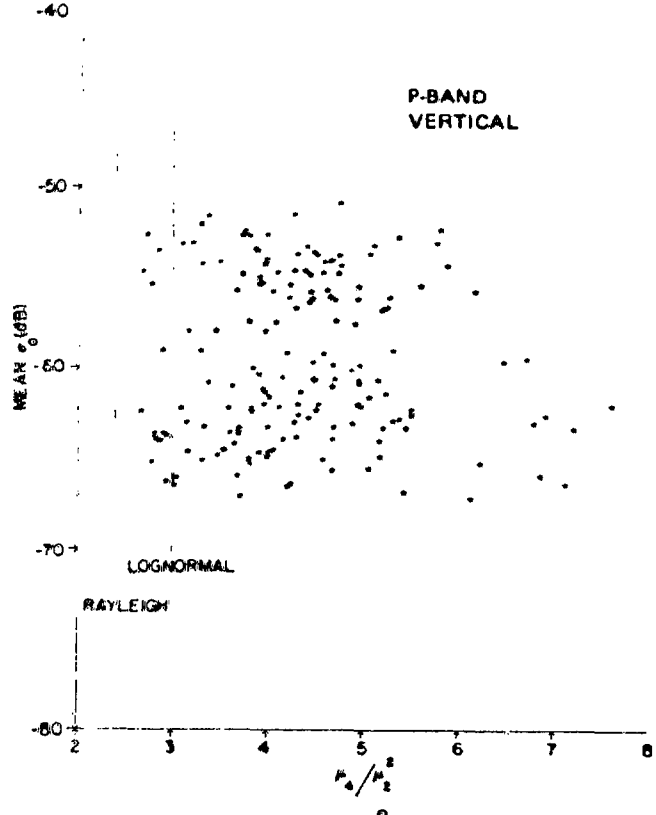

Fig. 41—The mean value vs μ_4/μ_2^2 of the normalized radar cross section of terrain clutter (in decibel units)

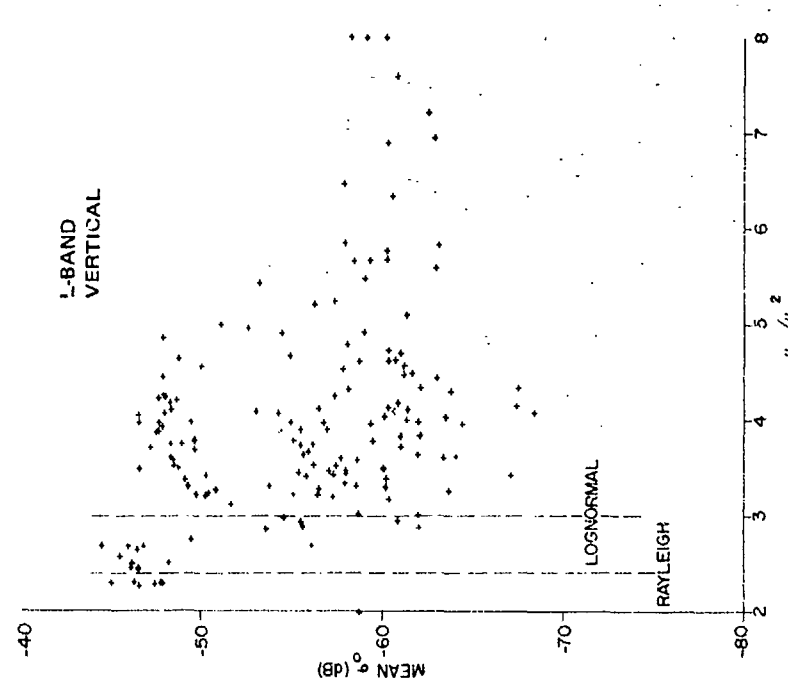

Fig. 43—The mean value vs μ_4/μ_2^2 of the normalized radar cross section of terrain clutter (in decibel units)

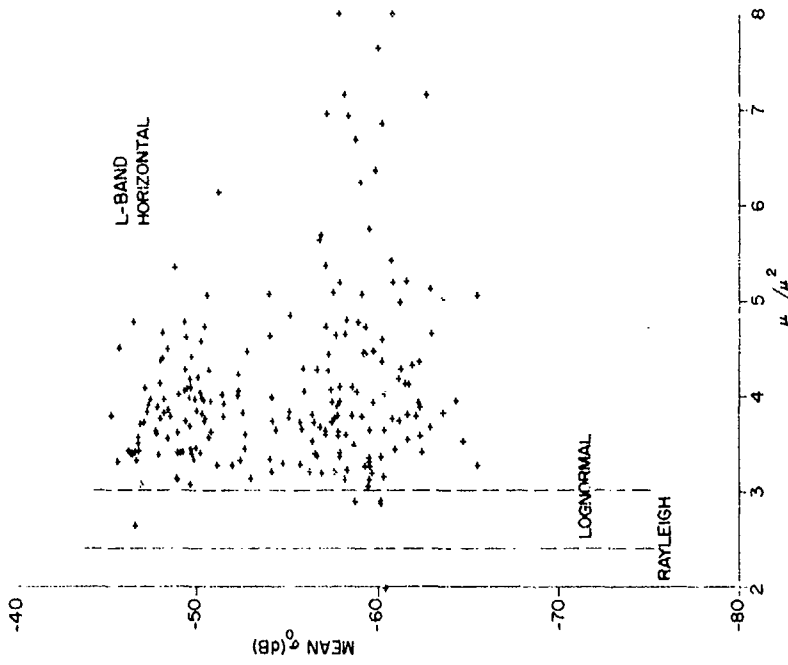

Fig. 42—The mean value vs μ_4/μ_2^2 of the normalized radar cross section of terrain clutter (in decibel units)

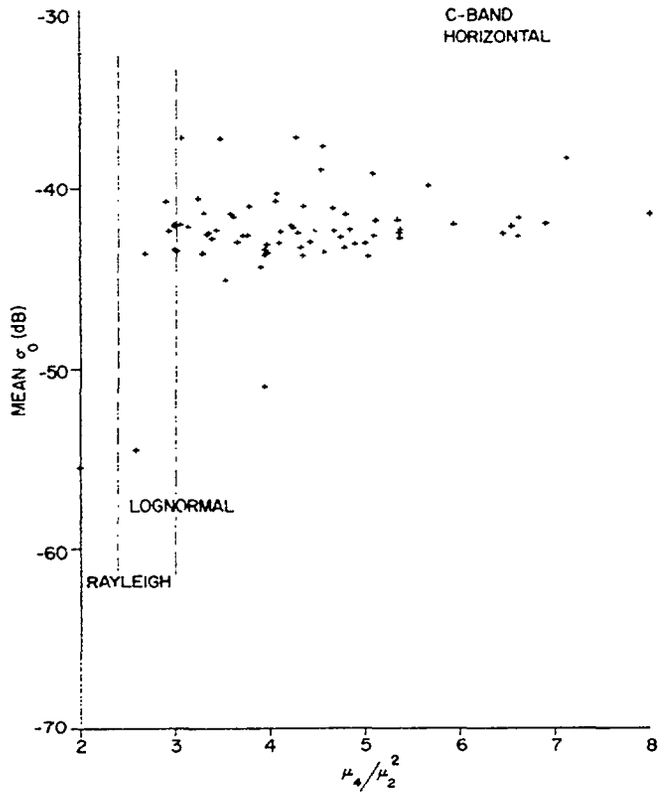

Fig. 44—The mean value vs μ_4/μ_2^2 of the normalized radar cross section of the terrain clutter (in decibel units)

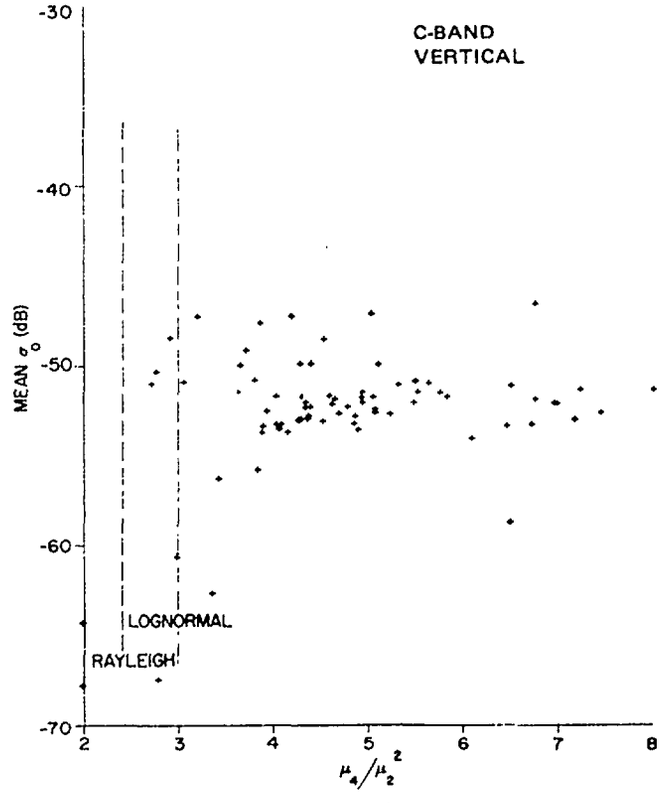

Fig. 45—The mean value vs μ_4/μ_2^2 of the normalized radar cross section of terrain clutter (in decibel units)

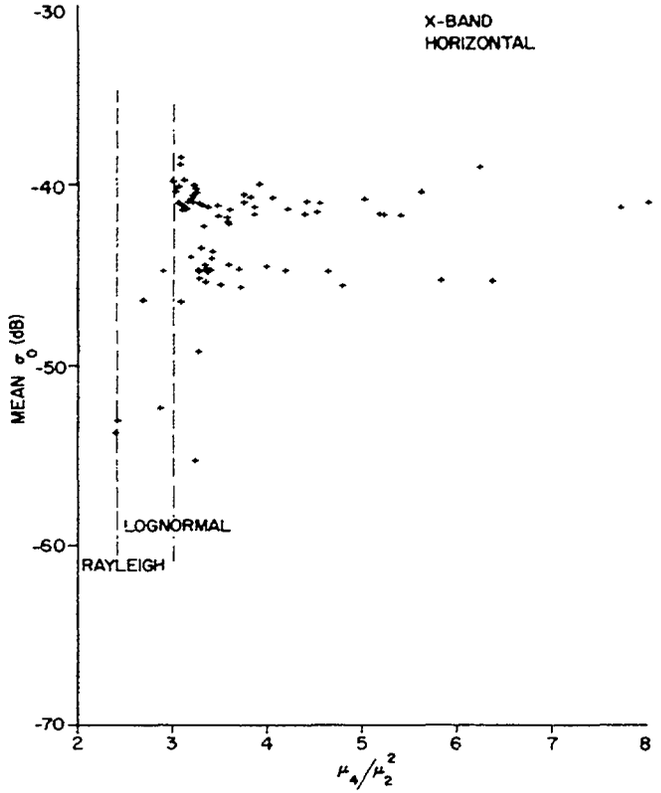

Fig. 46—The mean value vs μ_4/μ_2^2 of the normalized radar cross section of terrain clutter (in decibel units)

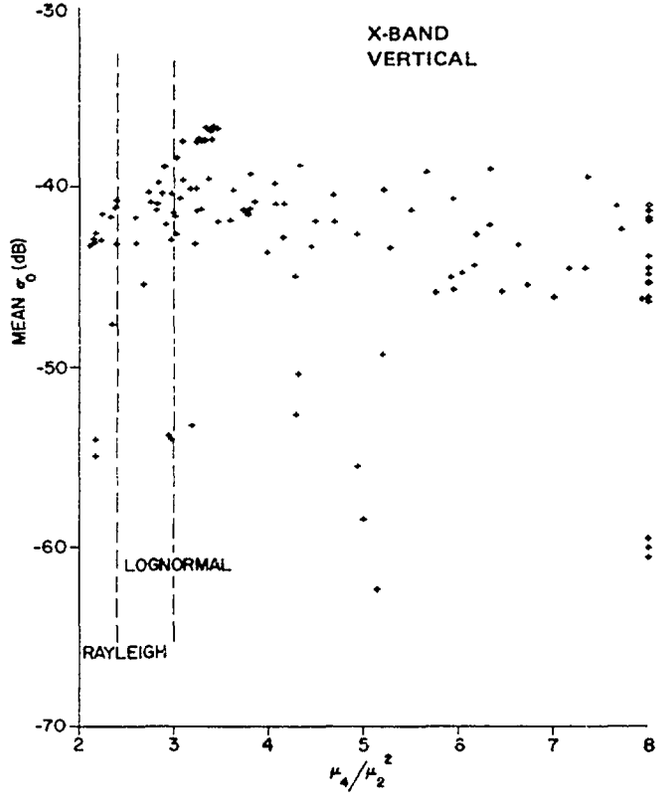

Fig. 47—The mean value vs μ_4/μ_2^2 of the normalized radar cross section of terrain clutter (in decibel units)

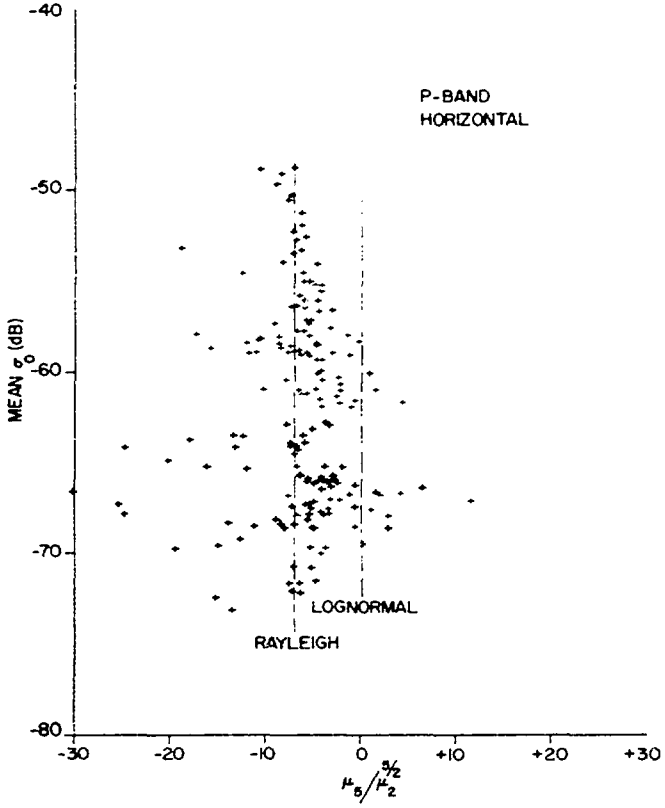

Fig. 48—The mean value vs $\mu_5/\mu_2^{5/2}$ of the normalized radar cross section of terrain clutter (in decibel units)

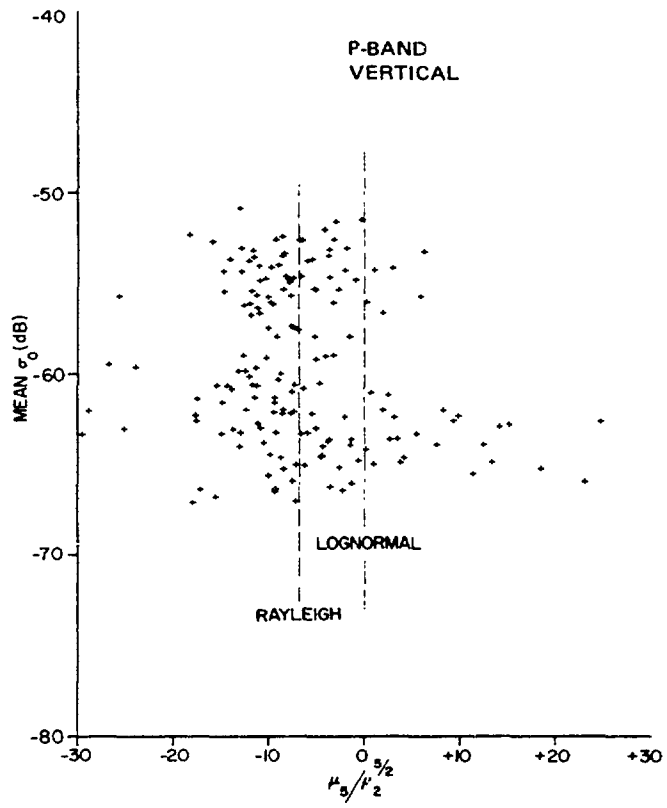

Fig. 49—The mean value vs $\mu_5/\mu_2^{5/2}$ of the normalized radar cross section of terrain clutter (in decibel units)

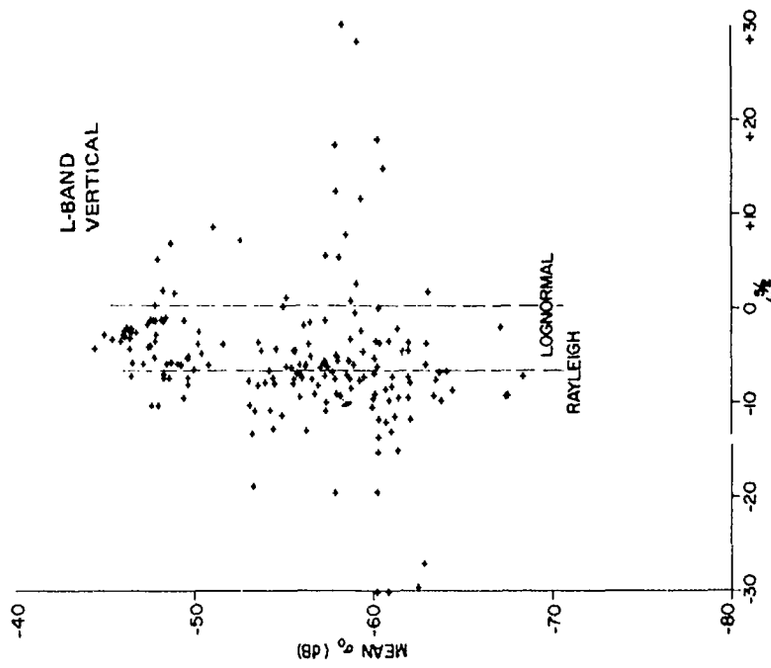

Fig. 51—The mean value vs $\mu_5/\mu_2^{5/2}$ of the normalized radar cross section of terrain clutter (in decibel units)

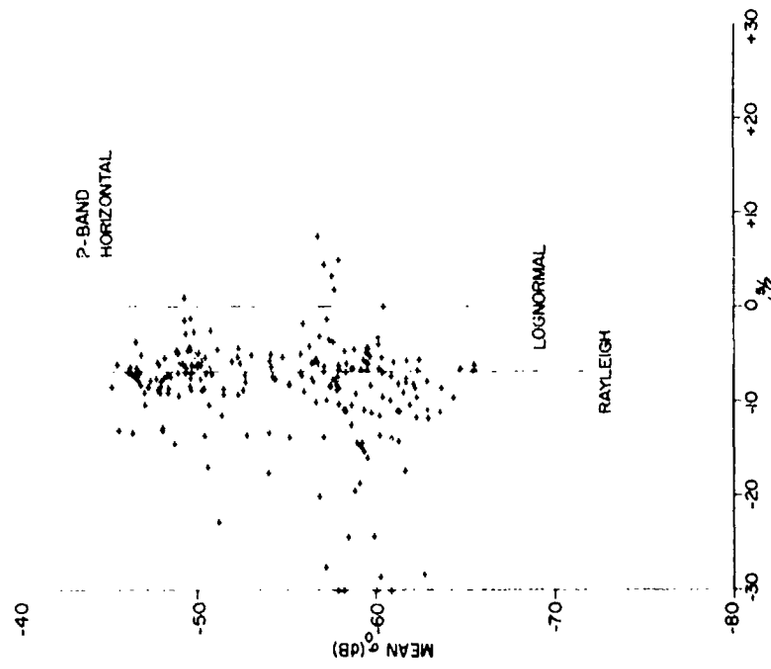

Fig. 50—The mean value vs $\mu_5/\mu_2^{5/2}$ of the normalized radar cross section of terrain clutter (in decibel units)

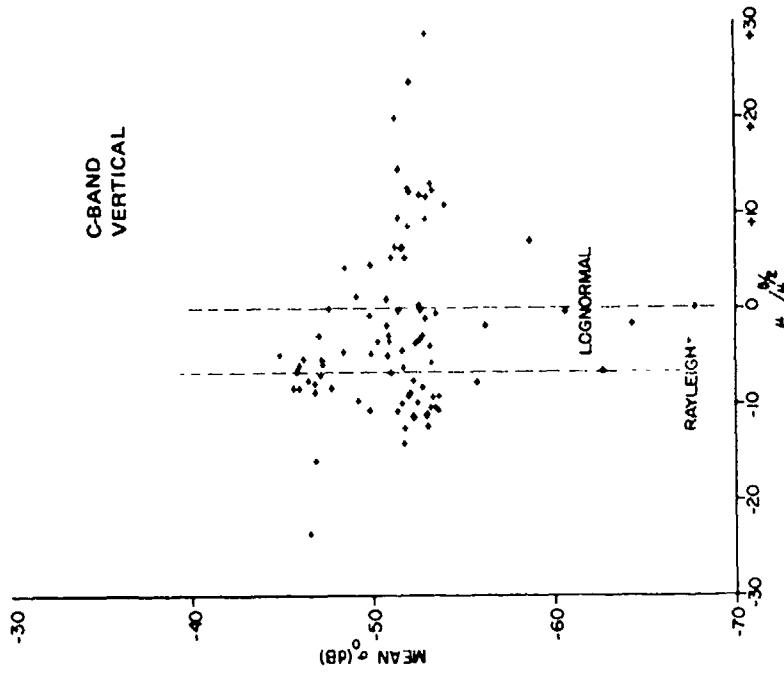

Fig. 53—The mean value vs $\mu_5/\mu_2^{5/2}$ of the normalized radar cross section of terrain clutter (in decibel units)

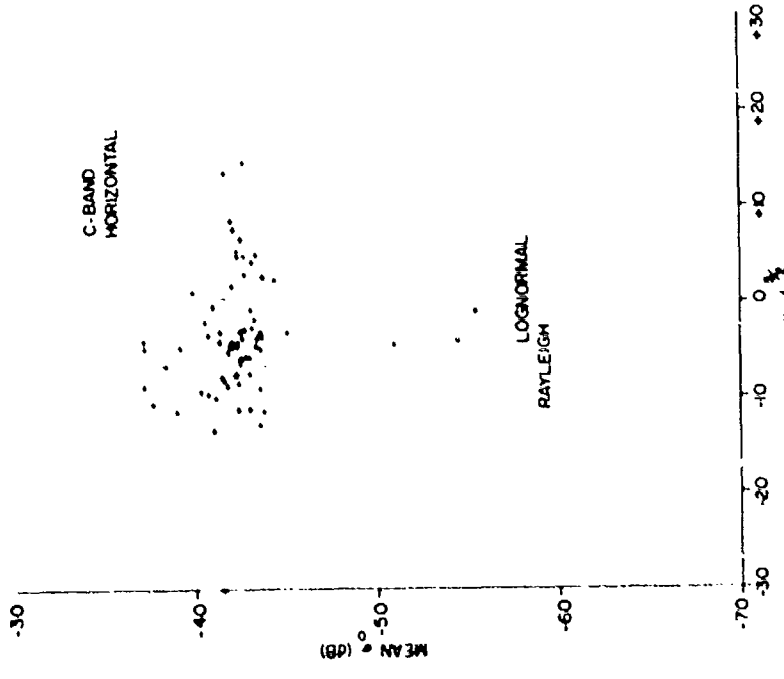

Fig. 52—The mean value vs $\mu_5/\mu_2^{5/2}$ of the normalized radar cross section of terrain clutter (in decibel units)

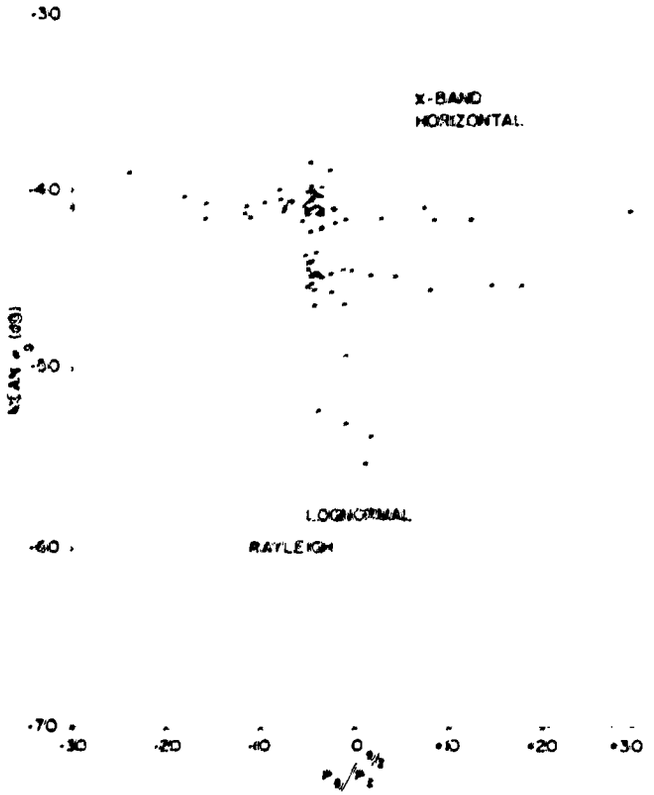

Fig. 54—The mean value vs $\mu_5/\mu_2^{5/2}$ of the normalized radar cross section of terrain clutter (in decibel units)

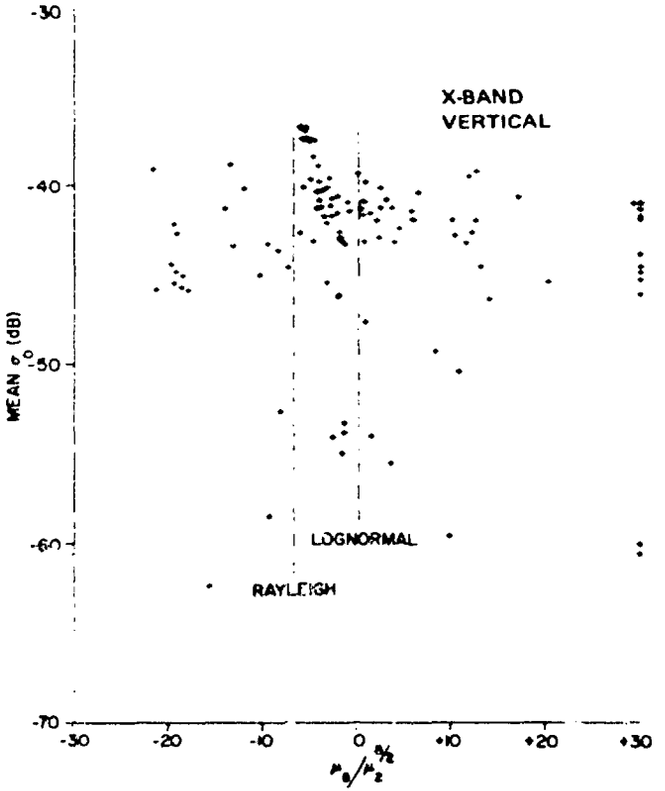

Fig. 55—The mean value vs $\mu_5/\mu_2^{5/2}$ of the normalized radar cross section of terrain clutter (in decibel units)

of lognormal distributions, and for these cases the tail of the distributions may be approximated by a lognormal distribution.

Of course, in order to evaluate fully the merits of the point-scatterer formulation for the statistics of terrain clutter a great deal of further investigation of the statistics of data is required.

ACKNOWLEDGMENT

The point-scatterer formulation for the statistics of terrain clutter evolved during the years in which the Electormagnetic Scattering Branch (formerly the Wave Propagation Branch) has collected terrain clutter data. This model was proposed by N. W. Guinard to whom we are most grateful, for this, and for many fruitful exchanges of ideas during this investigation.

REFERENCES

1. Guinard, N.W., Ransone, J.T., Jr., Laing, M.B., and Hearton, L.E., "NRL Terrain Clutter Study, Phase I," NRL Report 6487, May 10, 1967.
2. Blau, W., and Farber, J., "Radar Clutter Modeling," Spectronics Inc., Report TR 68-053, Contract N00014-68-C-0120, Nov. 1968.
3. Harger, R.O., "Synthetic Aperture Radar Systems: Theory and Design," New York, Academic Press, 1970.
4. Klauder, J.R., Price, A.C., Darlington, S., and Albersheim, W.J., "The Theory and Design of Chirp Radars," Bell Syst. Tech. J. 39 (No. 4), 745-808 (July 1960).
5. Cox, C., and Munk, W., "Slopes of the Sea Surface Deduced from Photographs of Sun Glitter," Bull. Scripps Inst. Oceanogr. 6 (No. 9), 401-488 (Sept. 1956).
6. Gnedenko, B.V., and Kolmogorov, A.N., "Limit Distributions for Sums of Independent Random Variables," 1968 ed., transl. K.L. Chung, Reading, Mass., Addison-Wesley.
7. Bernstein, S., "Sur l'extension du théorème limite du calcul des probabilités aux sommes des quantités dépendantes," Math. Ann. 97, 1-59 (1926).
8. Rice, S.O., "Mathematical Analysis of Random Noise," Bell Syst. Tech. J. 23, 282-332 (1944) and 24, 46-156 (1945).
9. Rice, S.O., "Statistical Properties of a Sine Wave plus Random Noise," Bell Syst. Tech. J. 27, 109-157 (1948).
10. Middleton, D., "An Introduction to Statistical Communication Theory," New York, McGraw-Hill, 1960.
11. Beckmann, P., "Rayleigh Distribution and its Generalizations," J. Res. NBS, Radio Sci. 68D (No. 9), 927-932 (Sept. 1964).
12. Daley, J.C., Davis, W.T., Duncan, J.R., and Laing, M.B., "NRL Terrain Clutter Study, Phase II," NRL Report 6749, Oct. 21, 1968.
13. Massey, F.J., Jr., "The Kolmogorov-Smirnov Test for Goodness of Fit," J. Am. Stat. Assoc. 46, 68-78 (1951).

14. Bendat, J.S., and Piersol, A.G., "Measurement and Analysis of Random Data," New York, Wiley, 1966.

15. Weinstock, W., "Target Cross Section Models for Radar Systems Analysis," Ph.D. Dissertation, University of Pennsylvania, Philadelphia, 1964.

16. Davis, H.T., "Tables of the Mathematical Functions," rev. ed., vol. II, San Antonio, Texas, The Principia Press of Trinity University, 1963.

17. Valenzuela, G.R., and Laing, M.B., "On the Statistics of Sea Clutter," NRL Report 7349, Dec. 30, 1971.